Chapter 7

Recent Progress in AlGaN Deep-UV LEDs

Hideki Hirayama

Additional information is available at the end of the chapter

http://dx.doi.org/10.5772/intechopen.79936

Abstract

AlGaN deep ultraviolet light-emitting diodes (DUV LEDs) have a wide variety of potential applications, including uses for sterilization, water purification, and UV curing and in the medical and biochemistry fields. However, the wall-plug efficiency (WPE) of AlGaN DUV LEDs remains below values. We have developed crystal growth techniques for wide-bandgap AlN and AlGaN and, using these techniques, fabricated DUV LEDs in the 220–350 nm-band. Considerable increases in the internal quantum efficiency (IQE) of AlGaN quantum wells (QW) were achieved by developing low-threading dislocation density (TDD) AlN grown on sapphire substrates. The electron injection efficiency (EIE) was substantially increased by introducing a multi-quantum barrier (MQB) as an electron-blocking layer (EBL). The light-extraction efficiency (LEE) was also improved by using a transparent p-AlGaN contact layer, a highly reflective (HR) p-type electrode, and an AlN template fabricated on a patterned sapphire substrate (PSS). Further improvements were made by implementing a reflective photonic crystal (PhC) p-contact layer. We demonstrated a record external quantum efficiency (EQE) of 20.3% for an AlGaN UVC-LED.

Keywords: deep-UV LEDs, AlN, AlGaN, MOCVD, threading-dislocation density, internal quantum efficiency, light-extraction efficiency

1. Introduction

Growth techniques for AlN/AlGaN semiconductors and recent advances in AlGaN-based deep-ultraviolet (DUV) light-emitting diodes (LEDs) are demonstrated. DUV LEDs operating in the 220–350-nm band were realized by developing new crystal growth techniques for the wide-bandgap semiconductors, AlN and AlGaN. The efficiency of an AlGaN DUV LED was significantly increased through past 10 years developments, by increasing in internal quantum efficiency (IQE), which was achieved by developing low threading dislocation density (TDD)

AlN crystals on sapphire substrates, as well as, by improving electron injection efficiency (EIE) and light extraction efficiency (LEE).

In Section 2, the background to this research, including device applications, history and the current status of DUV LEDs, is described. In Section 3, we describe the development of the crystal growth techniques undertaken in order to obtain high-quality AlN and AlGaN crystals. The realization of devices with high IQE and fabrication of the LEDs are dealt with in Sections 4 and 5, respectively. We discuss ways in which EIE and LEE can be improved, and the future prospects for DUV LEDs, in Sections 6, 7 and 8, respectively.

2. Research background of UV LEDs

The development of semiconductor light sources operating in the DUV region, such as DUV LEDs and laser diodes (LDs), is an important subject because these devices are required for a wide variety of applications. **Figure 1** gives an overview of these applications, divided into three wavebands. Potential applications for UVC and UVB lights are in sterilization, water purification, medicine and biochemistry, agriculture, and as light sources for high-density optical memory. UVA together with UVB and UVC lights also have potential for curing, adhesives, printing and coating [1, 2].

Figure 2 shows the wavelength range of UV light from UVA to UVC, and possible wavelength range of DUV LEDs developed by AlGaN. As well known, UVA light causes sunburn and UVB light is dangerous light, which causes skin cancer or cataracts. Indicated curve in **Figure 2** with peak wavelength at 265 nm in UVC waveband is known as sterilization effects curve, which well matches to the absorption spectrum of DNA (deoxyribonucleic acid). The wavelength between 260 and 280 nm is effective for sterilization, water purification and surface

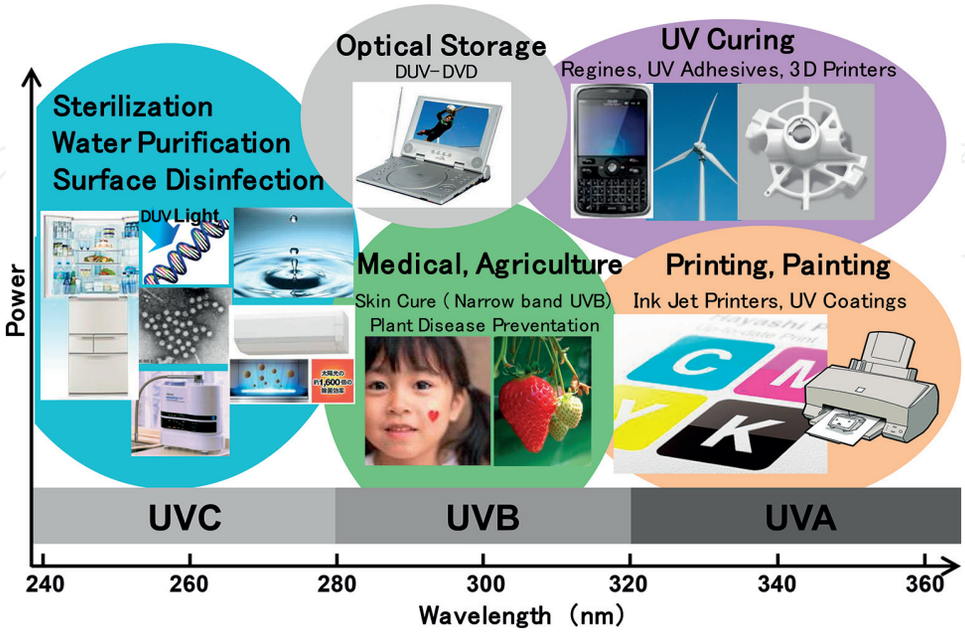

Figure 1. Potential applications of DUV LEDs and LDs.

http://dx.doi.org/10.5772/intechopen.79936

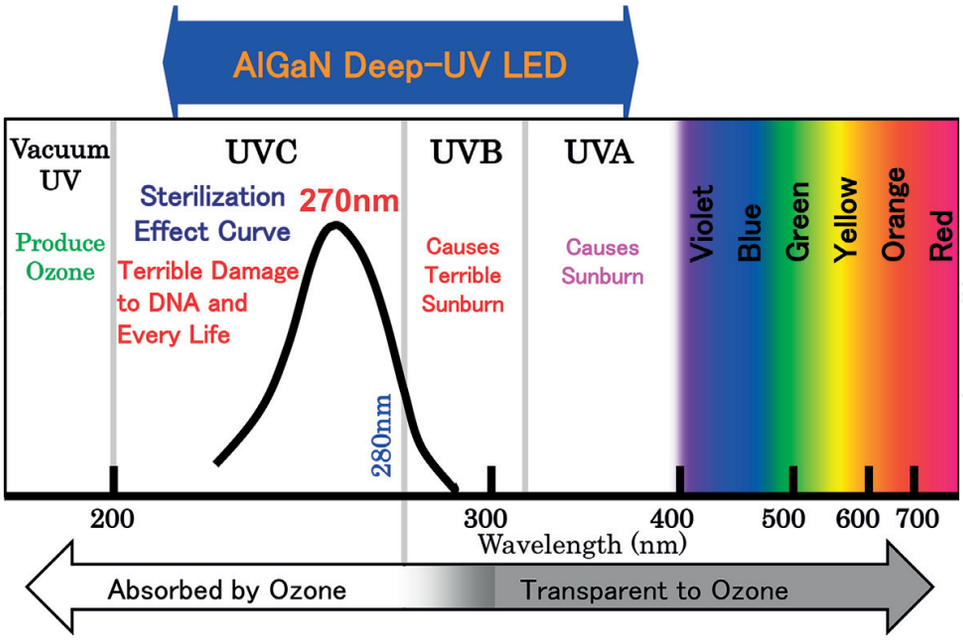

Figure 2. Classification of UV light and the wavelength range achieved by AlGaN DUV LEDs.

disinfection. As shown in **Figure 2**, the wavelength range covered by AlGaN LEDs is from UVA to UVC.

The direct transition energy range of AlGaN covers the region from 6.2 eV (AlN) to 3.4 eV [2]. **Figure 3** shows the bandgap of the wurtzite (WZ) AlInGaN material system, as well as, the lasing wavelengths of several kinds of gas lasers. AlGaN is a direct transition semiconductor having an emission wavelength range from 200 to 360 nm. Both p- and n-type conductivities are obtained in DUV wavelength range. AlGaN is physically hard and suitable for long lifetime devices. Also, the material is free from harmful elements, i.e., As, Hg and Pb. Therefore, AlGaN is considered to be the most appropriate semiconductor to develop a DUV LED [2].

Several research groups have started the research on AlGaN-based UV LEDs with wavelength below 360 nm, between 1996 and 1999 [3–5]. In the US, the effort, directed at DUV light sources, was driven by DARPA's Semiconductor Ultraviolet Optical Sources (SUVOS) program. The sub-300 nm DUV LEDs were achieved by a group at the University of South Carolina between 2002 and 2006 [6–8]. The shortest wavelength (210 nm) LED using an AlN emitting layer was reported by a group at NTT in 2006 [9]. We started research into AlGaN-based DUV LEDs in 1997, and reported the first efficient DUV (230 nm) photoluminescence (PL) from AlGaN/AlN QWs [10], and a 330 nm-band AlGaN-QW UV LED on SiC in 1999 [4]. We have also developed highly efficient UV LEDs by incorporating In into AlGaN [1, 11, 12]. We demonstrated cw operation with powers of several mWs for 340–350 nm InAlGaN-QW UV LEDs on both GaN single-crystal substrates [13] and sapphire substrates [14].

The development of 260–280 nm AlGaN DUV LEDs performed in 2005–2010 was an important step in the progress toward sterilization applications. High IQEs in AlGaN and quaternary InAlGaN QWs were achieved in 2007 [15–17], by developing a low-threading dislocation density (TDD) AlN buffer layers on sapphire substrates utilizing a pulse-flow growth method. EIE was significantly increased by introducing a multi-quantum barrier (MQB) [18]. Wide

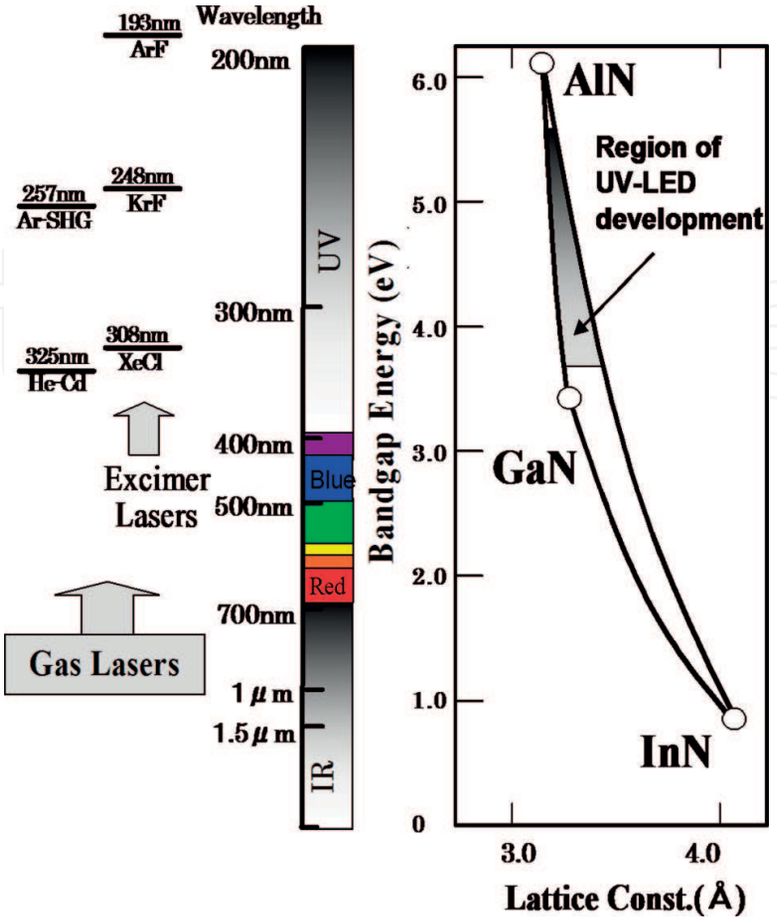

Figure 3. Relationship between the direct transition bandgap energy and the lattice constant of the wurtzite (WZ) InAlGaN material system and the lasing wavelengths of various gas lasers.

range emissions from 222 to 351 nm were demonstrated in AlGaN and InAlGaN LEDs [17–21]. We began to improve LEE of UVC LEDs by introducing a transparent p-AlGaN contact layer and a reflective p-type electrode [22–24]. We also developed commercially available DUV LED modules to be used for sterilization in 2014 [25, 26].

Sensor Electronic Technology (SET) developed the first commercially available LEDs with wavelengths ranging between 240 and 360 nm [27–28]. They reported a maximum EQE of 11% for a 278 nm LED in 2012 [28]. They also did detailed investigations into the properties of AlGaN epilayers and UVC LED devices [29–31].

Since 2010, many companies have started developing UVC LEDs aiming at sterilization applications. Nikkiso has developed highly efficient UVC LEDs [32–34] and reported EQEs of over 10% [32]. They improved the LED properties by introducing an encapsulating resin that does not deteriorate under UVC radiation [34]. Crystal IS developed efficient 265 nm LEDs on bulk AlN substrates fabricated by a sublimation method [35, 36], and Tokuyama developed UVC LEDs on a thick transparent AlN layer grown, also on bulk AlN substrates, by hydride vapor phase epitaxy (HVPE) [37–40]. Nichia has developed high wall-plug efficiency (WPE) UVC LEDs [41, 42] using a lens bonding technique [42]. Also, M. Kneissl's group in the Technical

University of Berlin recently carried out a series of studies on the properties of AlGaN epilayers and AlGaN and InAlGaN UV LEDs [2, 43–45]. The reported EQEs for AlGaN and InAlGaN UVA-UVC LEDs up to 2015 are summarized in Figure 1.1 of Ref. [2].

In spite of continuous efforts to develop an AlGaN DUV LED, its wall plug efficiency (WPE) is still as low as 3%, which is much lower than that of InGaN blue LEDs. The limited efficiency of DUV LED is mainly due to the following three factors:

1. The IQE of AlGaN is sensitive to TDD and still much lower than that of InGaN.
2. Hole concentration of p-AlGaN is low and the carrier injection efficiency (IE) is low.
3. By the light absorption by p-GaN contact layer, the LEE is quite low.

For InGaN QWs, high IQE more than 80% was already demonstrated. On the other hand, IQE at around 50% is standard value after developing the low-TDD (5×10^8 cm^{-2}) AlN templates on sapphire. We need to develop further reduction of TDD of AlN, i.e. TDD of below 1×10^8 cm^{-2}, in order to achieve more than 80% IQE. AlN single crystal wafers have advantages for high IQE, although they are expensive for commercially available DUV LEDs. The hole concentration of p-AlGaN used in UVC LEDs is as low as 1×10^{14} cm^{-3} owing to its deep acceptor levels, i.e., 240 (GaN)–590 meV (AlN). Electron overflow to the p-side layers results in the reduction of EIE for UVC LEDs. Since the hole density of p-type AlGaN is not very high, we use p-GaN for the contact layer. This results in a significant reduction in LEE, typically to below 8%, owing to the strong absorption of DUV light.

The usual value of EQE for 270 nm UVC LEDs obtained by our group is approximately 7%, which is determined by the IQE, EIE, and LEE of approximately 60, 80, and 15%, respectively. The technical issues to increase IQE, EIE and LEE are described in the following sections.

3. Growth of high-quality AlN on sapphire substrates

In order to obtain low-TDD, crack-free AlN buffer layer with atomically flat surface on sapphire, we introduced an 'ammonia (NH_3) pulsed-flow multilayer (ML) growth method [15]. **Figure 4** shows a schematic view of the growth control method and a typical gas flow sequence using pulsed and continuous gas flows.

The samples were grown on sapphire (0001) substrates at 76 Torr by metal-organic chemical vapor deposition (MOCVD). First, an AlN nucleation layer and a 'buried' AlN layer were deposited, both by NH_3 pulsed-flow growth. The pulsed-flow mode is effective for initial high-quality AlN growth on sapphire because of the increased migration of the precursor. After the growth of the first layers, we introduced a continuous-flow mode AlN growth to reduce the surface roughness. By repeating the pulsed- and continuous-flow modes, we can obtain crack-free, thick AlN layers with atomically flat surfaces. By maintaining Al-rich growth conditions, we can obtain stable Al (+c) polarity, which is necessary for suppressing polarity inversion from Al to N. The detailed growth conditions are described in Ref. [15, 19]. The advantages in comparison with former approaches [46, 47] are that the method is in-situ

process, and low TDD AlN can be obtained without the need for AlGaN layers, yielding a device structure with minimal DUV absorption.

Figure 5 shows the full-width at half maximum (FWHM) of X-ray diffraction (10–12) ω-scan rocking curves (XRC) for various stages in the ML-AlN growth. This was reduced from 2160 to 550 arcsec by executing the pulsed-flow mode twice. **Figure 6** shows atomic-force microscope

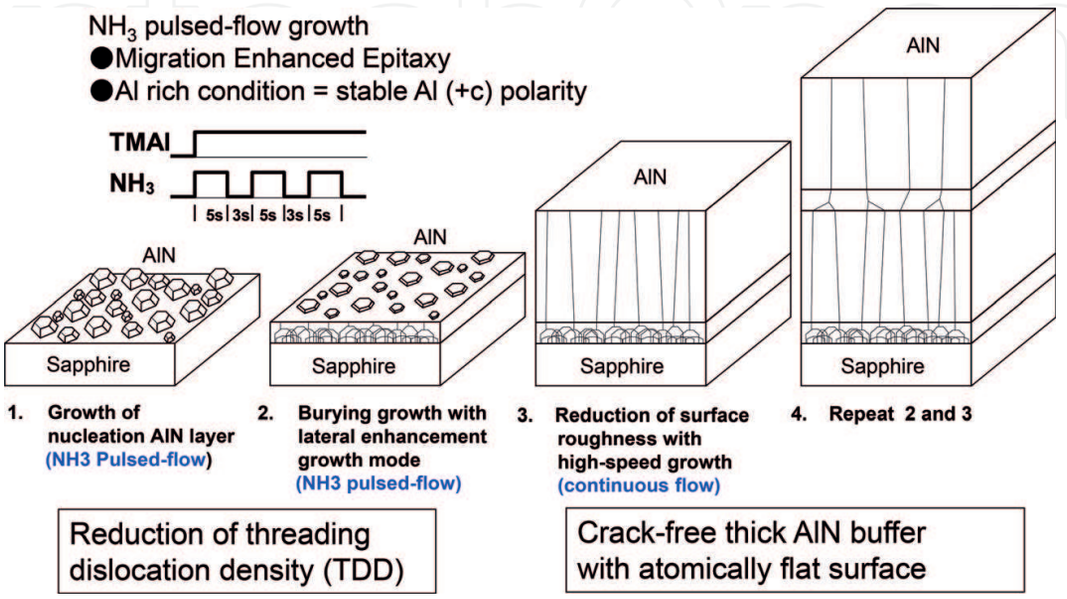

Figure 4. Gas flow sequence and schematic view of the growth control method used for the NH_3 pulsed-flow multilayer (ML)-AlN growth technique.

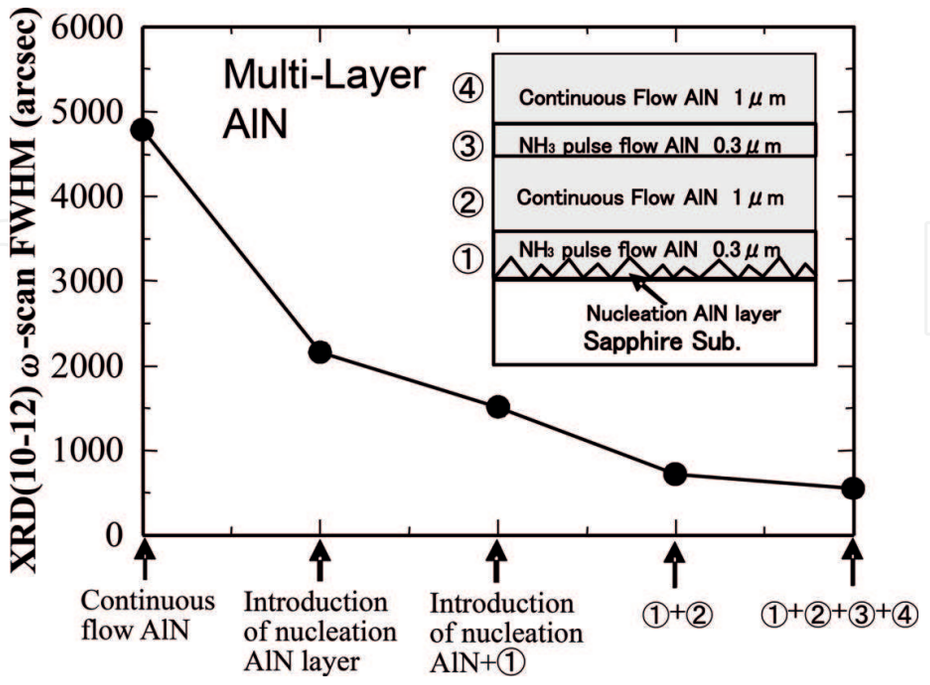

Figure 5. FWHM of the X-ray diffraction (10–12) ω-scan rocking curve (XRC) at various stages in the growth of the ML-AlN layer.

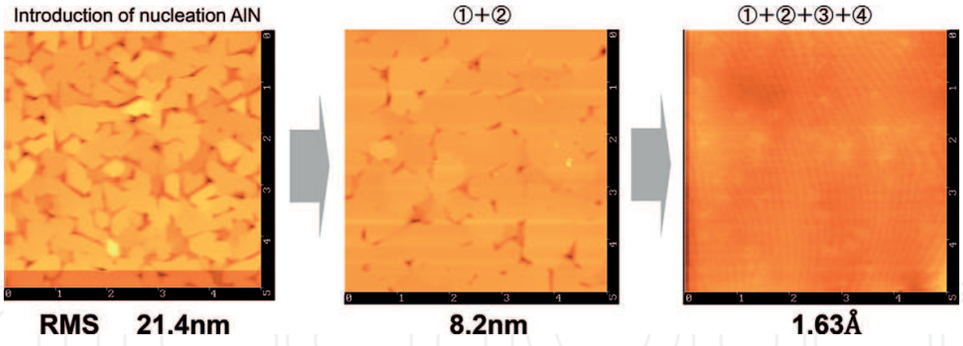

Figure 6. AFM images of the surface of the ML-AlN layer with an area of 5 × 5 μm^2 at various stages in the growth.

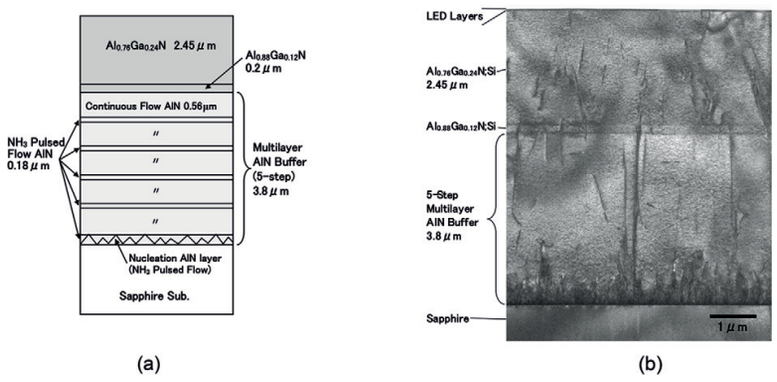

Figure 7. (a) Schematic diagram and (b) cross-sectional TEM image of an AlGaN/AlN template including a 5-step ML-AlN buffer layer grown on a sapphire substrate.

(AFM) images of the surface of ML-AlN on sapphire at various stages of growth. We can see that the surface improves as more layers are grown, ending with an atomically flat surface. The typical root-mean-square (RMS) of the surface roughness was 0.16 nm, as seen in **Figure 6**.

Figure 7 shows (a) a schematic illustration of the structure and (b) a cross-sectional transmission electron microscope (TEM) image of an AlGaN/AlN template including ML-AlN buffer layer grown on a sapphire substrate. The typical FWHMs of the (10–12) and (0002) XRCs of the ML-AlN were approximately 330 and 180 arcsec, respectively. This was grown in a 3 × 2 inch MOCVD reactor [25]. The minimum corresponding FWHMs obtained using a 1 × 2 inch MOCVD reactor were approximately 290 and 180 arcsec, respectively. The minimum edge- and screw-type dislocation densities were below 5 × 10^8 and 4 × 10^7 cm^{-2}, respectively, as observed in the TEM image. To further reduction of TDD, we introduced an AlN epitaxial lateral overgrowth (ELO) technique on a patterned sapphire substrate (PSS) and obtained TDDs of the order of 10^7 cm^{-2}.

4. Increasing the internal quantum efficiency (IQE)

Figure 8 shows a cross-sectional TEM image of an AlGaN multi-quantum well (MQW) of a 227 nm DUV LED fabricated on a ML-AlN buffer. In order to suppress the spontaneous

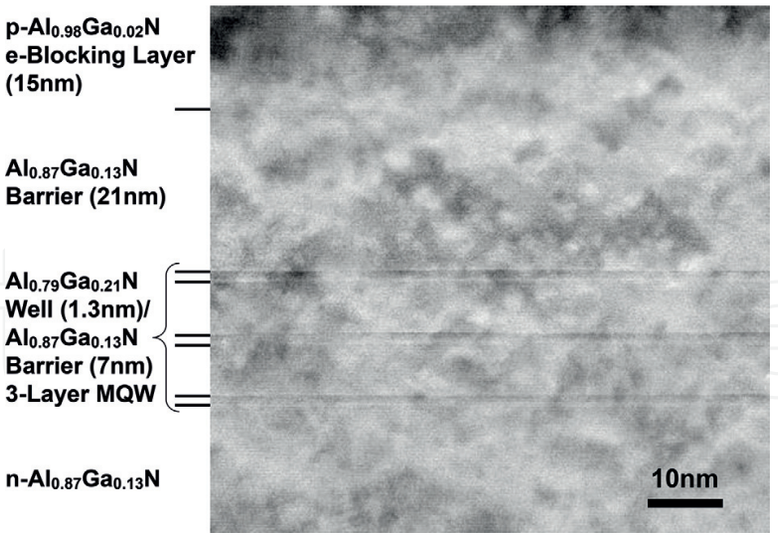

Figure 8. Cross-sectional TEM image of the quantum well region of an AlGaN MQW DUV-LED.

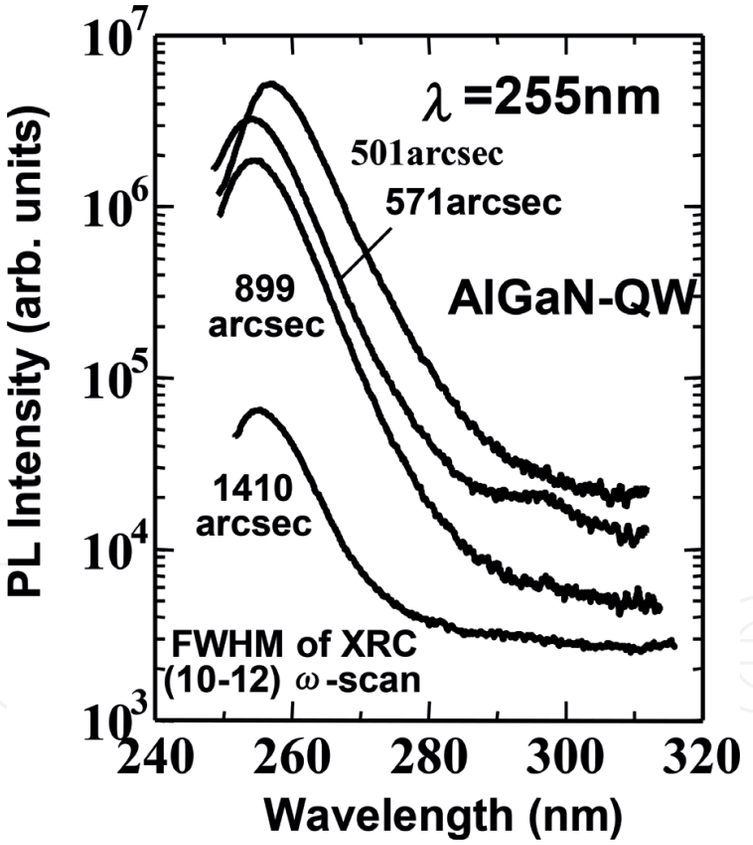

Figure 9. Photoluminescence (PL) spectra of AlGaN QWs on ML-AlN templates with various FWHMs of the XRC (10–12) measured at room temperature.

polarization effects induced in the wells, very thin quantum well was used. It is important to obtain atomically smooth hetero-interfaces to achieve high IQE from such thin QWs. As shown in the cross-sectional TEM image in **Figure 8**, the three 1.3 nm-thick QWs have atomically-flat hetero-interfaces.

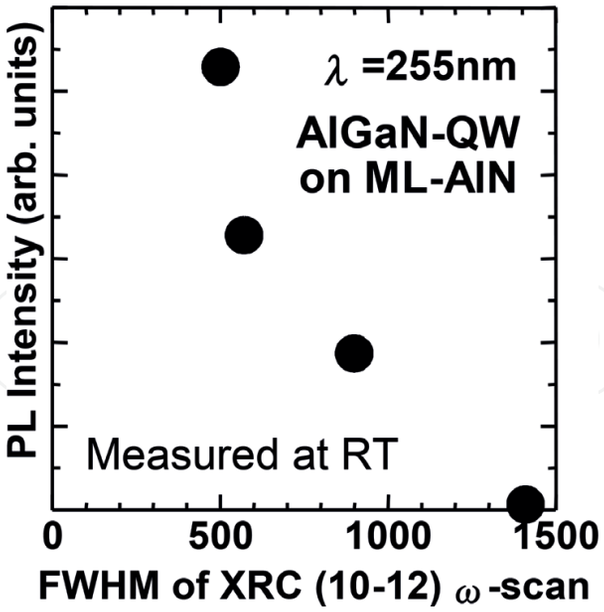

Figure 10. PL intensity of AlGaN-QWs as a function of the FWHM of the XRC (10–12) of AlGaN buffers measured at room temperature.

We observed a considerable increase in the DUV emission from AlGaN-QWs by fabricating them on low TDD AlN templates [16, 17]. **Figure 9** shows the photoluminescence (PL) spectra of AlGaN QWs with emission peaks at around 255 nm fabricated on ML-AlN measured at room temperature (RT). We used a 244 nm Ar-ion second-harmonics generation (SHG) laser for the excitation of the sample. The excitation power density was approximately 200 W/cm^2. The PL intensity significantly increases with narrower FWHM. We can see from **Figure 9** that the efficiency depends strongly on the edge-type TDDs.

Figure 10 shows the intensity of the PL peak at 255-nm measured at RT as a function of the FWHM of the XRC (10–12). Reducing the FWHM from 1400 to 500 arcsec increases the PL intensity by a factor of about 80. Between 500 and 800 arcsec the PL intensity increases rapidly. This rapid increase can be explained by a reduction in the non-radiative recombination rate as the distance between the TDs becomes greater compared with the carrier diffusion length in the QW. We obtained similar degrees of improvement for QWs operating at other wavelengths. The relationship between IQE and TDD in DUV AlGaN-QWs was also investigated in Ref. [27, 48].

The quaternary alloy InAlGaN is also a strong candidate as a material for realizing DUV LEDs, since the inclusion of In leads to efficient UV emission as well as higher hole concentration. Just a few percent of In in AlGaN is needed to obtain high IQE, where the increases in efficiency are due to the In segregation effect, an effect previously investigated for the ternary alloy, InGaN. We have described the advantages of the use of InAlGaN in Ref. [1, 11, 12, 14, 17].

We took up the challenge of developing the crystal growth technology needed to obtain high quality InAlGaN alloys operating at the 'sterilization' wavelength (280 nm) [17]. Growing crystals of InAlGaN with a high Al content is relatively difficult, because incorporating In becomes more challenging as the growth temperature is increased, which is necessary in order

to maintain the crystal quality. We obtained high-quality InAlGaN with a high amount of Al (>45%) by using epitaxy at a relatively low growth rate, i.e., 0.03 μm/h. The intensity of the light at 280 nm emitted by an InAlGaN QW at RT was increased by a factor of 5 by reducing the growth rate from 0.05 to 0.03 μm/h.

5. AlGaN- and InAlGaN-based UVA-UVC LEDs

We fabricated AlGaN and InAlGaN MQW DUV LEDs on low-TDD AlN templates [15–26]. **Figure 11** shows a schematic diagram of the structure of an AlGaN-based DUV LED fabricated on a sapphire substrate. **Table 1** shows typical design values for the fraction of Al (x) in the $Al_xGa_{1-x}N$ wells, in the buffer and barrier layers, and in the electron-blocking layers (EBLs) used for 222–273 nm AlGaN-MQW LEDs. Large compositions of Al in AlGaN were used to obtain DUV LEDs operating at short wavelengths, as shown in **Table 1**. The detail layer structures and device geometries of the LEDs are described in Ref. [15, 17]. The output power was measured using a Si photodetector located behind the LED sample. The photodetector was calibrated by measuring the luminous flux from a flip-chip LED. The forward voltages

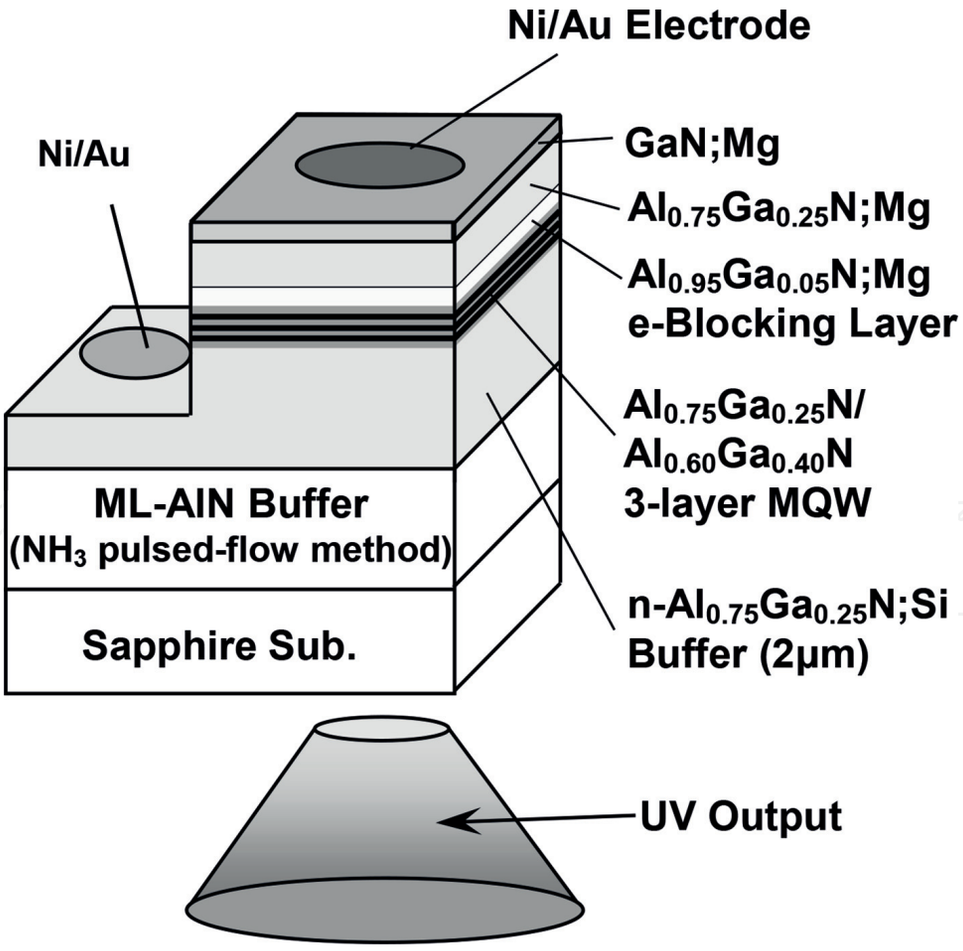

Figure 11. Schematic structure of a typical AlGaN-based DUV LED fabricated on a sapphire substrate.

Wavelength	Well	Barrier & Buffer	Electron Blocking Layer
222 nm	0.83	0.89	0.98
227 nm	0.79	0.87	0.98
234 nm	0.74	0.84	0.97
248 nm	0.64	0.78	0.96
255 nm	0.60	0.75	0.95
261 nm	0.55	0.72	0.94
273 nm	0.47	0.67	0.93

Table 1. Typical design values of the fraction of Al (x) in the $Al_xGa_{1-x}N$ wells, the buffer and barrier layers, and the electron-blocking layers (EBLs) used for 222–273 nm AlGaN-MQW LEDs.

(Vf) of the bare wafer and the flip-chip samples were approximately 15 and 8 V, respectively, with an injection current of 20 mA.

Figure 12 shows the electroluminescence (EL) spectra of the AlGaN and InAlGaN MQW LEDs measured at RT. We obtained single-peak operations for LED samples with emission wavelength from 222 to 351 nm. **Figure 13** shows the EL spectra of a 227 nm AlGaN LED on a log scale [19]. The deep-level emissions with wavelengths at around 255 and 330–450 nm are more

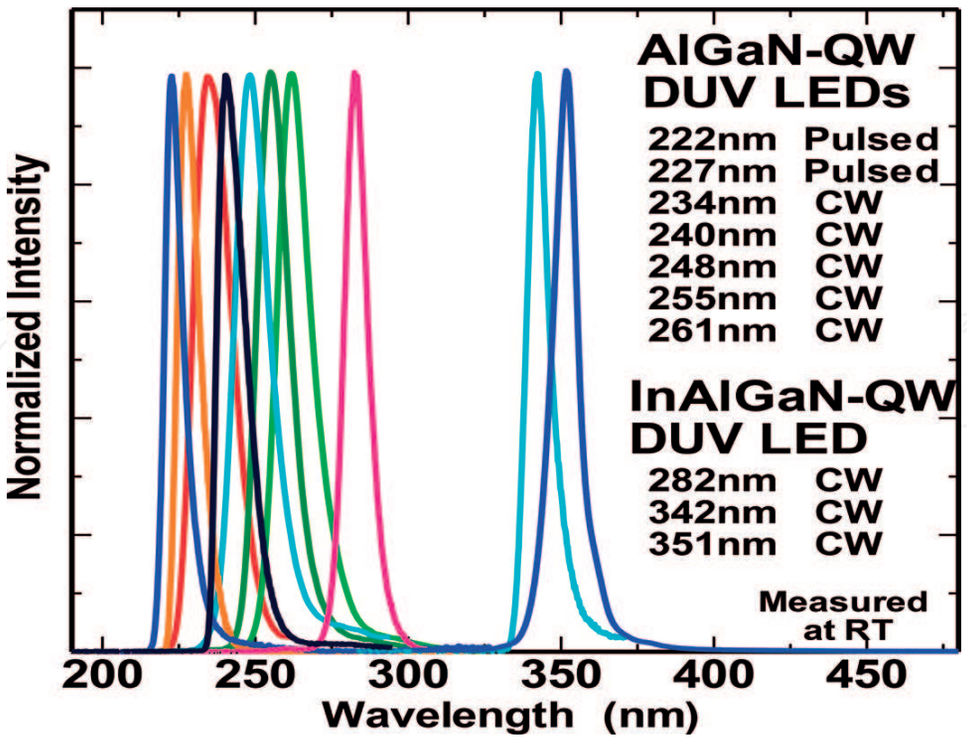

Figure 12. Electroluminescence (EL) spectra of fabricated AlGaN and InAlGaN MQW LEDs with emission wavelengths between 222 and 351 nm, all measured at room temperature (RT) with injection currents of around 50 mA.

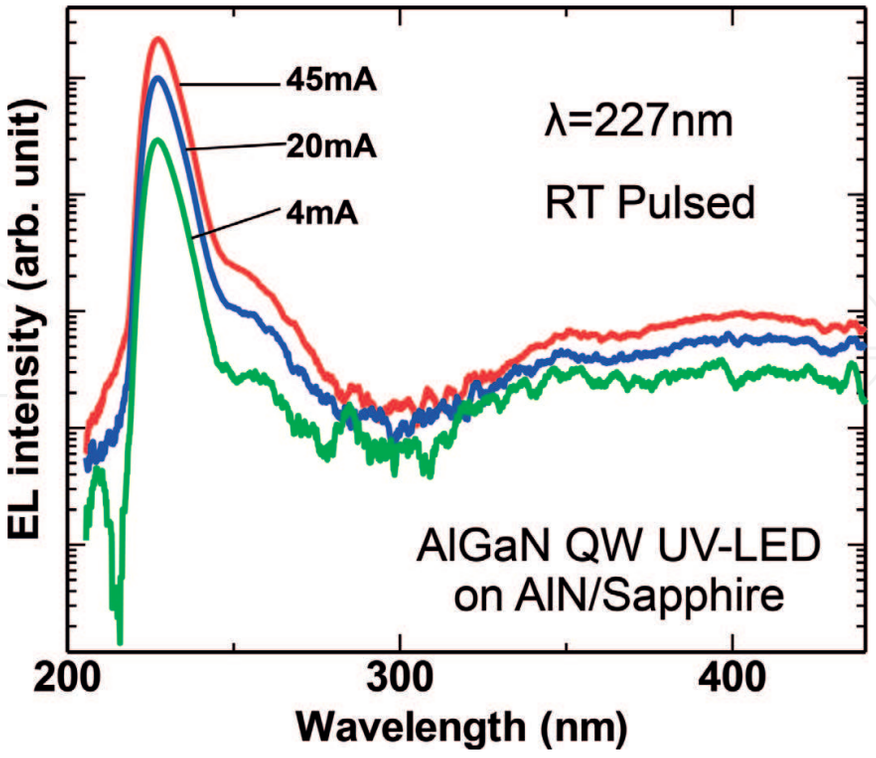

Figure 13. EL spectra on a log scale of a 227 nm AlGaN DUV LED for various injection currents.

than two orders of magnitude smaller than the main peaks. The output power of the 227 nm LED was 0.15 mW at an injection current of 30 mA, and the maximum EQE was 0.2% under pulsed operation at RT. **Figure 14** shows (a) the EL spectra for various injection currents and (b) the current-output power (I-L) and current-EQE (η_{ext}) (I-EQE) characteristics for a 222 nm AlGaN-MQW LED measured under pulsed operation at RT [20]. Single-peak operation at

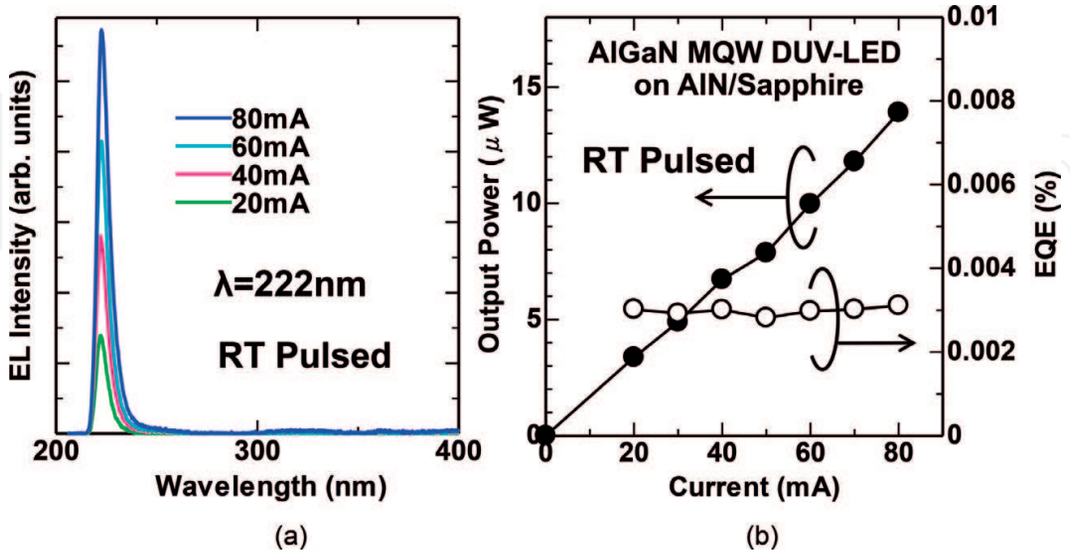

Figure 14. (a) EL spectra for various injection currents and (b) the output power and EQE (η_{ext}) *vs* current characteristics for a 222 nm AlGaN-MQW LED measured under pulsed operation at RT.

222 nm, which is the shortest wavelength ever reported for a QW LED, was achieved. The output power was 0.14 μW at an injection current of 80 mA, and the maximum EQE was 0.003%.

It has been reported that 'normal' c-axis (vertical) emission is difficult to obtain from an AlN (0001). This is because the optical transition between the conduction band and the top of the valence band is mainly only allowed for light that has its electric field parallel to the c-axis (E//c) [9]. The lateral propagation of the transvers-magnetic (TM) mode emission results in a significant reduction of LEE. Therefore, short wavelength AlGaN UVC LED shows a very low LEE. Several groups have reported on this [49, 50]. Banal et al. reported that the critical Al composition for 'polarization switching' could be expanded to approximately 0.82 by using very thin (<1.5 nm) AlGaN quantum wells on an AlN/sapphire template [49]. We investigated the variation in the spectrum of a 222 nm AlGaN QW LED with the angle of emission, and demonstrated that normal vertical emission can be obtained, even at short-wavelengths, for LEDs with as much as 83% Al [20].

6. Increasing the electron injection efficiency (EIE) by introducing an MQB

EIE into the QW is reduced due to the electron leakage caused by the low hole concentrations in the p-type AlGaN layers. The EIE reduction is particularly severe for LEDs with wavelength shorter than 260 nm, because an electron barrier height of an EBL becomes smaller [17]. We introduced a MQB [51, 52] to serve as an EBL, and consequently achieved a marked increase in EIE [18].

Figure 15 shows schematic illustrations of the electron flow for an AlGaN DUV LED with (a) a MQB EBL and (b) a conventional single barrier EBL. In usual case, we are using single barrier EBL for 250–280 nm UVC LEDs. However, the electron barrier height of the single barrier EBL is determined by the bandgap of the barrier material, and it is not sufficiently high for UVC LED with wavelength shorter than 260 nm. On the other hand, we can increase the 'effective' barrier height of the EBL by introducing MQB. Even electrons having higher energy above the MQB band-edge can be reflected by the multi-reflection effects of the MQB, and injected into the QWs, resulting in higher EIE.

Figure 16 shows the electron transmittance through an AlGaN MQB and a conventional single barrier EBL for a 250 nm AlGaN LED calculated by a transfer-matrix method. It was shown, using barriers with thickness modulation, that the 'effective' barrier height of an AlGaN/AlGaN MQB is up to twice that of a conventional single-barrier EBL.

Figure 17 shows a schematic diagram of the structure of a 250 nm AlGaN QW DUV LED with an MQB EBL and a cross-sectional TEM image of a fabricated device. We carried out experiments to find an appropriate MQB structure, and found that the insertion of an initial thick-barrier is important for reflecting low energy electrons. We also found that thin barriers contribute to the reflection of higher-energy electrons. The optimum MQB comprised five layers of $Al_{0.95}Ga_{0.05}N/Al_{0.77}Ga_{0.23}N$ with thicknesses of **7**/4/**5.5**/4/**4**/2.5/**4**/2.5/**4** nm, in which

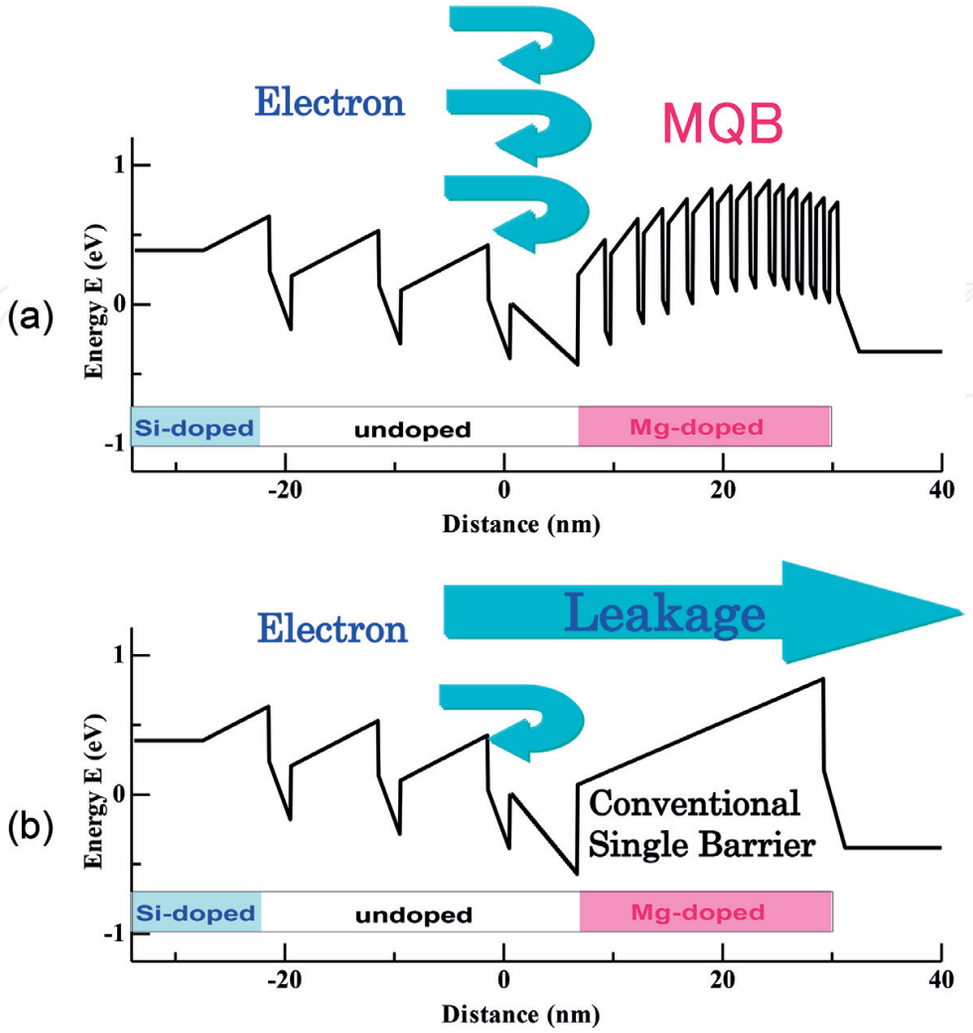

Figure 15. Schematic images of the electron flow in AlGaN DUV LEDs with (a) a MQB EBL and (b) a conventional single barrier EBL.

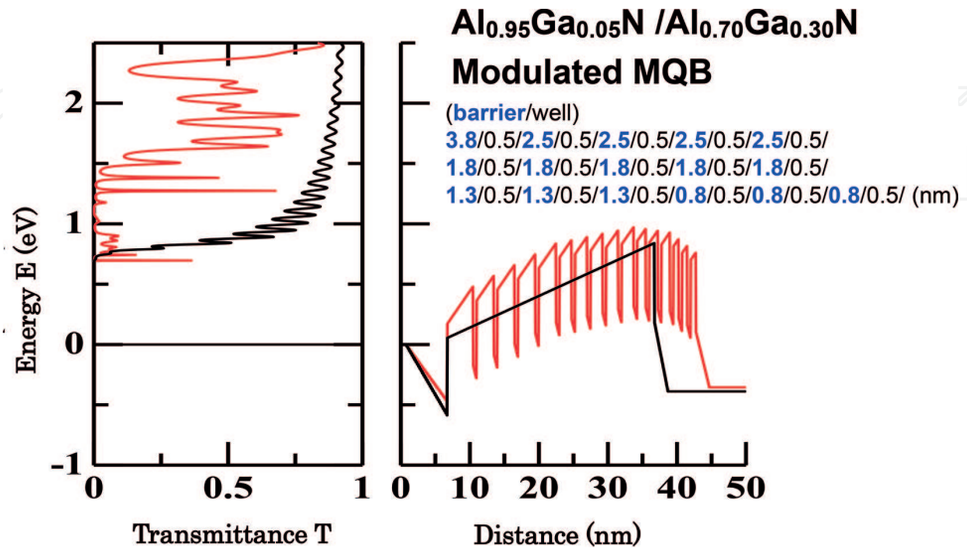

Figure 16. Electron transmittance through AlGaN/AlGaN MQB (red-line) and conventional single barrier EBL (black-line) calculated for a 250 nm-band AlGaN-QW LED.

http://dx.doi.org/10.5772/intechopen.79936

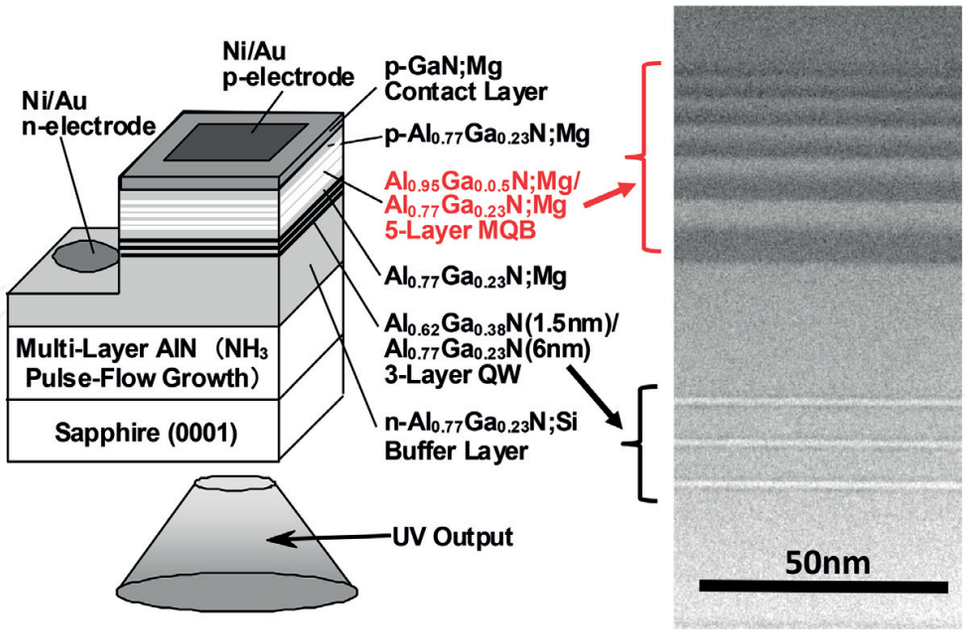

Figure 17. Schematic structure and cross-sectional TEM image of a 250 nm AlGaN QW DUV LED with an MQB.

the barriers are in bold type and the valleys are normal type. The coherence length for obtaining the multi-reflection effect of the MQB means the total thickness of the MQB should be less than 40 nm.

Figure 18 shows (a) the I-L and (b) I-EQE characteristics for 250 nm AlGaN MQW LEDs with an MQB and with a single-barrier EBL, both measured under cw operation at RT. These show significant increases in output power and EQE when the single-EBL is replaced by the MQB. The maximum output powers of LEDs with the MQB and with the single-barrier EBL are 15 mW and 2.2 mW, respectively, and the introduction of the MQB has increased the EQE by a

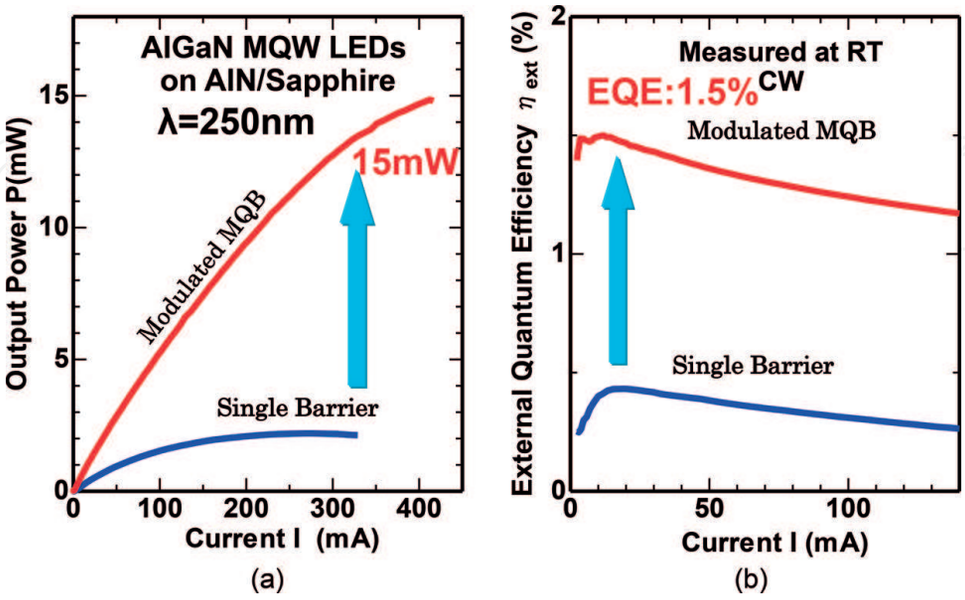

Figure 18. (a) Current-output power (I-L) and (b) current-EQE (η_{ext}) characteristics for 250 nm AlGaN-MQW LEDs with an MQB and with a single-EBL.

factor of approximately 4. From **Figure 18**, we estimate that the EIE would have been improved from approximately 25% to more than 80% by introducing the MQB.

Figure 19 shows the I-L characteristics for a 237 nm AlGaN MQW LED with an MQB and a 234 nm LED with a single-barrier EBL, both measured under cw operation at RT. The increase in EIE when using the MQW was found to be extremely high. The output power has been increased by a factor of 12 by replacing the single-barrier EBL with a MQB.

Figure 20 shows the wavelength dependence of the EQE for AlGaN DUV LEDs with MQBs and single-barrier EBLs. Introducing the MQB has increased the EQE by 10, 4 and 3 times for 235, 250 and 270 nm AlGaN LEDs, respectively. We obtained a cw output power of 33 mW from a 270 nm AlGaN-MQW LED with an MQB on a bare chip, but expect to get higher output power by using flip-chip geometry and heat dissipation. The value of EQE was 3.8% in the absence of any means to increase LEE [21].

RIKEN and Panasonic have developed commercially available UVC LED modules for use in sterilization in 2014 [25, 26]. To develop commercially available devices with constant high EQEs and long device lifetimes, the reproducibility and uniformity of the AlN template and the AlGaN LED layer structure need to be maintained. Reproducibility is particularly difficult because the growth conditions are very sensitive to the vapor-reaction between NH_3 and TMAl induced by high growth temperatures (1250–1400°C). We achieved highly uniform ML-AlN templates on sapphire in a 3 × 2 inch MOCVD reactor using pulsed NH_3 flow. The

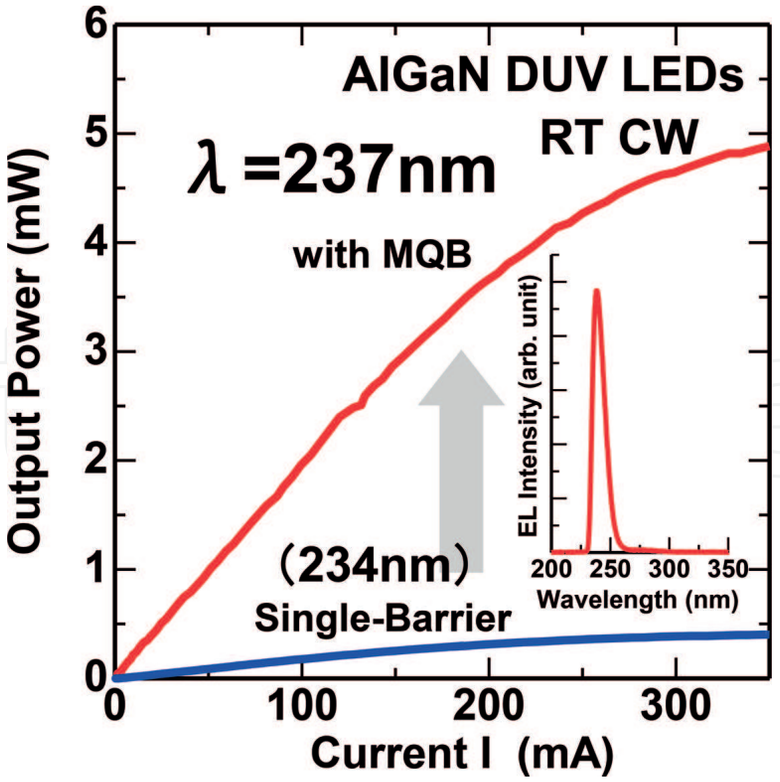

Figure 19. Current-output power (I-L) characteristics for a 237 nm AlGaN-MQW LED with an MQB and a 234 nm AlGaN-MQW LED with a single-EBL.

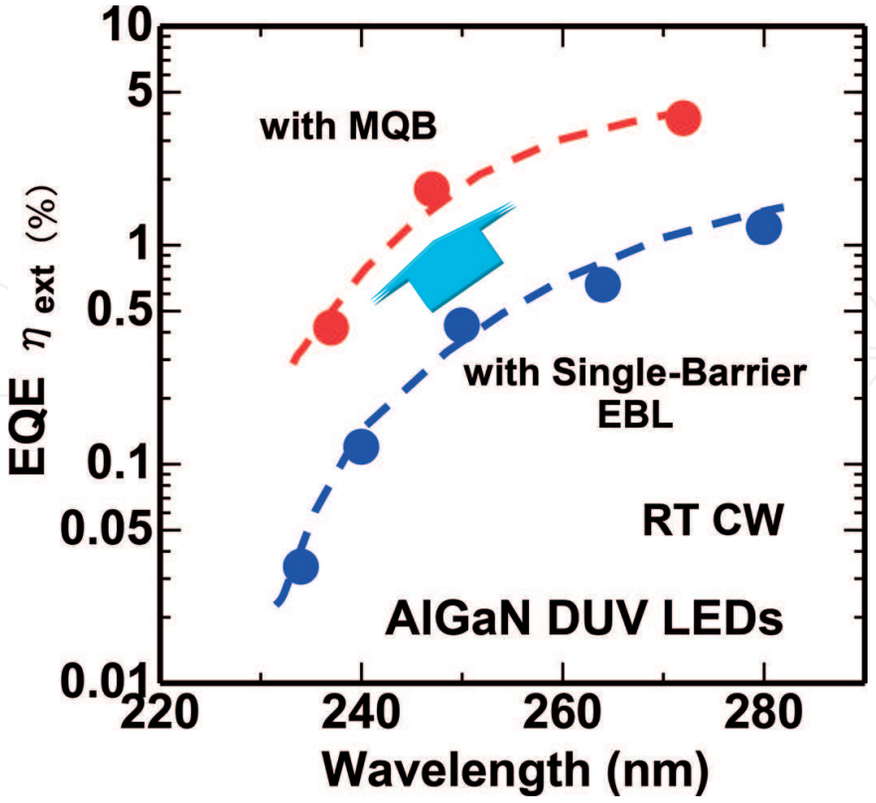

Figure 20. Wavelength dependence of the EQE of AlGaN DUV-LEDs with MQBs and single-EBLs.

fluctuation in FWHM for these was within 4%. We consistently obtained FWHMs of the XRC (10–12) of 340 arcsec for these templates. These highly uniform and low TDD templates are suitable for producing commercial DUV LEDs. **Figure 21** shows (a) a photograph of a 270 nm 10 mW DUV LED module containing 6 chips and (b) the operating properties of this module for applications to sterilization. Lifetimes longer than 10,000 h have already been achieved for devices with EQEs of 2–3% [25, 26].

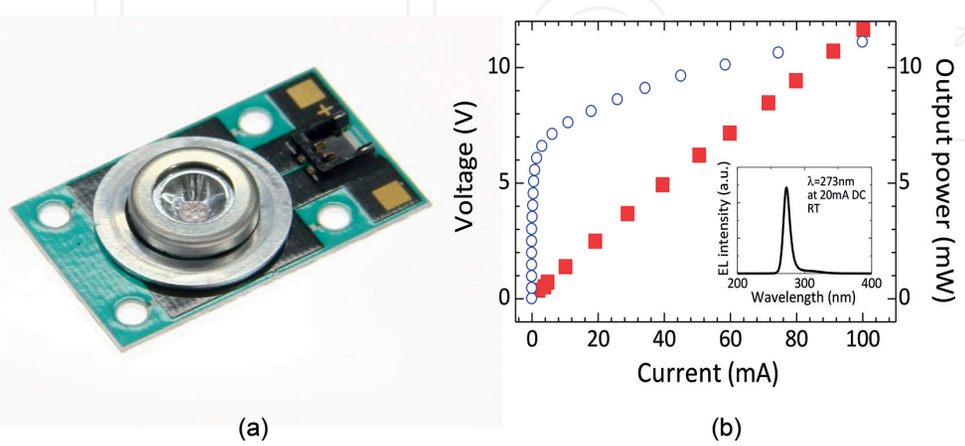

Figure 21. (a) Photograph of a commercially available 270 nm 10 mW DUV LED module developed by RIKEN and Panasonic for applications to sterilization and (b) the operating properties of this module.

7. Increasing the light-extraction efficiency (LEE)

Improving the LEE is particularly important for the development of AlGaN DUV LEDs, because LEE is currently quite low in comparison with that of InGaN-based blue LEDs. However, increasing LEE is not so easy because of the scarcity of suitable transparent, conducting p-type contact layers and transparent p-type electrodes, and also the lack of highly reflective p-type electrodes applicable to UVB-UVC range.

Figure 22 shows schematic diagrams of several structures designed to improve LEE, and the approximate values of LEE calculated for them [24]. In a conventional DUV LED, the light going upward from the QWs is completely absorbed by the p-GaN contact layer. The light going downward is reflected at the sapphire/air interface by total internal reflection. As a result, the LEE is less than 8%. Although we have used photonic nanostructures on the surface of the sapphire substrate or an encapsulating technique, the improvement in LEE is not sufficiently high (a maximum of approximately 15% is expected). To improve LEE, we must introduce a transparent contact layer and a highly reflective p-type electrode. If we use a transparent p-AlGaN contact layer and an electrode with a reflectivity of 80%, LEEs more than 20% can be obtained. Further improvements can be made from light scattering effects obtained by having an AlN buffer layer grown on a patterned sapphire substrate (PSS). LEEs of approximately 35% are expected by combining a transparent contact layer with a reflective electrode and a PSS. Yet more improvements can be made by having a vertical LED with a back-surface photonic structure, which can be realized by removing the sapphire substrate. LEEs of >70% are expected for such LEDs, as analyzed in Ref. [53]. We also proposed using a highly reflective (HR) PhC for the p-contact layer, as we discuss later, which has almost perfect reflectivity for UV light. Using a structure with a transparent p-AlGaN contact layer, a HR-PhC on p-AlGaN, and vertical geometry with a backside photonic patterned structure for light extraction, EQEs of more than 40% are expected for UVC LEDs.

We demonstrated a DUV LED with a transparent p-AlGaN contact layer and a reflective p-type electrode [24]. We replaced the conventional Ni (20 nm)/Au (100 nm) p-type electrode with a highly reflective Ni (1 nm)/Al (200 nm) electrode [54]. **Figure 23** shows the relative reflectivities of Ni/Al (200 nm) electrodes for various thicknesses of Ni (0.5–4 nm), and also that

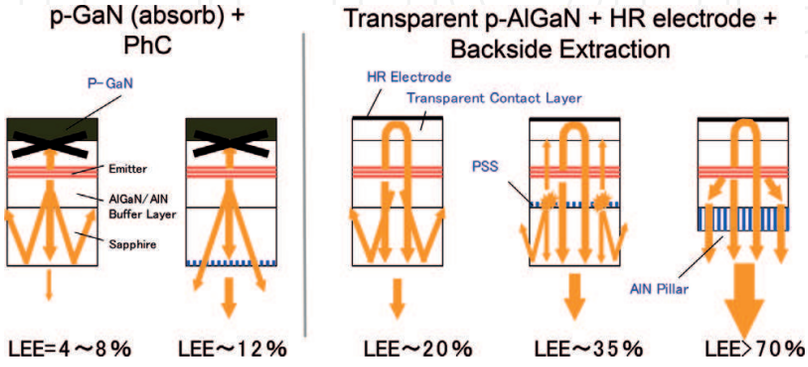

Figure 22. Schematic illustrations of structures designed to improve the LEE of a DUV LED and rough estimates of the values of LEE for each structure.

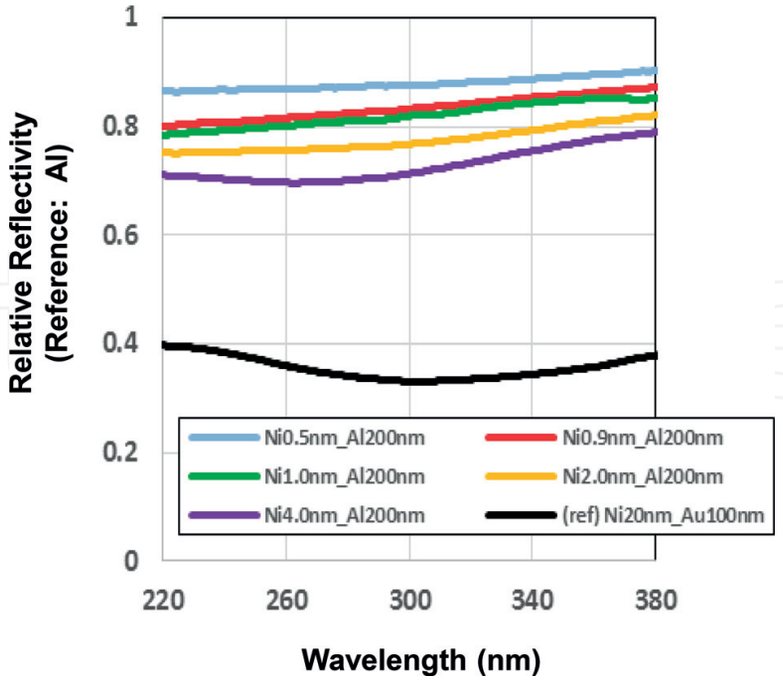

Figure 23. Wavelength dependence of the reflectivity for various types of p-type electrode for AlGaN DUV LEDs.

for Ni (20 nm)/Au (100 nm), normalized to the reflectivity of Al (92%). Although the reflectivity of Al metal is high (92%) in the DUV range, ohmic contact to p-AlGaN cannot be obtained. The insertion of a thin layer of Ni to improve this causes a significant reduction in reflectivity. Therefore, we did a thorough examination of the reflectivities of Ni/Al electrodes with very thin Ni layers. We confirmed normal operation of a UVC LED with a Ni (1 nm)/Al (200 nm) p-type electrode. The reflectivities of Ni (1 nm)/Al (200 nm) and Ni (20 nm)/Au (100 nm) electrodes are approximately 76 and 31%, respectively, as shown in **Figure 23**.

Figure 24 compares the effect of the different p-type electrodes on (a) the I-L and (b) the I-EQE characteristics of 279 nm AlGaN DUV LEDs with transparent p-AlGaN contact layers [54]. Using the highly reflective Ni(1 nm)/Al(200 nm) in place of the conventional Ni(20 nm)/Au(100 nm) electrode increases the EQE from 5 to 9% owing to the increase in LEE [54]. We also confirmed that Ni(1 nm)/Mg and rhodium (Rh) p-electrodes are effective to increase the LEE of UVC LED [55].

Increases in LEE were demonstrated for a 275 nm UVC flip-chip (FC) LED by using a transparent p-type AlGaN contact layer, an Rh mirror electrode, an AlN buffer layer grown on PSS, and an encapsulating resin. The effects of each of these were systematically investigated [56]. Conventional and LEE enhanced type LED structures were fabricated to investigate the effects of the aforementioned features on LEE. Schematics of these are shown in **Figure 25(a)** and **(b)**, respectively. The structures were grown by MOCVD for a conventional LED on a 4 μm thick AlN/sapphire template, and for a LEE enhanced type on an AlN/PSS. The detail layer and devise structures were described in Ref. [56].

Figure 26 shows a photograph of the FC LED sample. An Al-coated Si submount was used for the FC LED. The chip was encapsulated in hemispherical lens-like by silicon resin. We

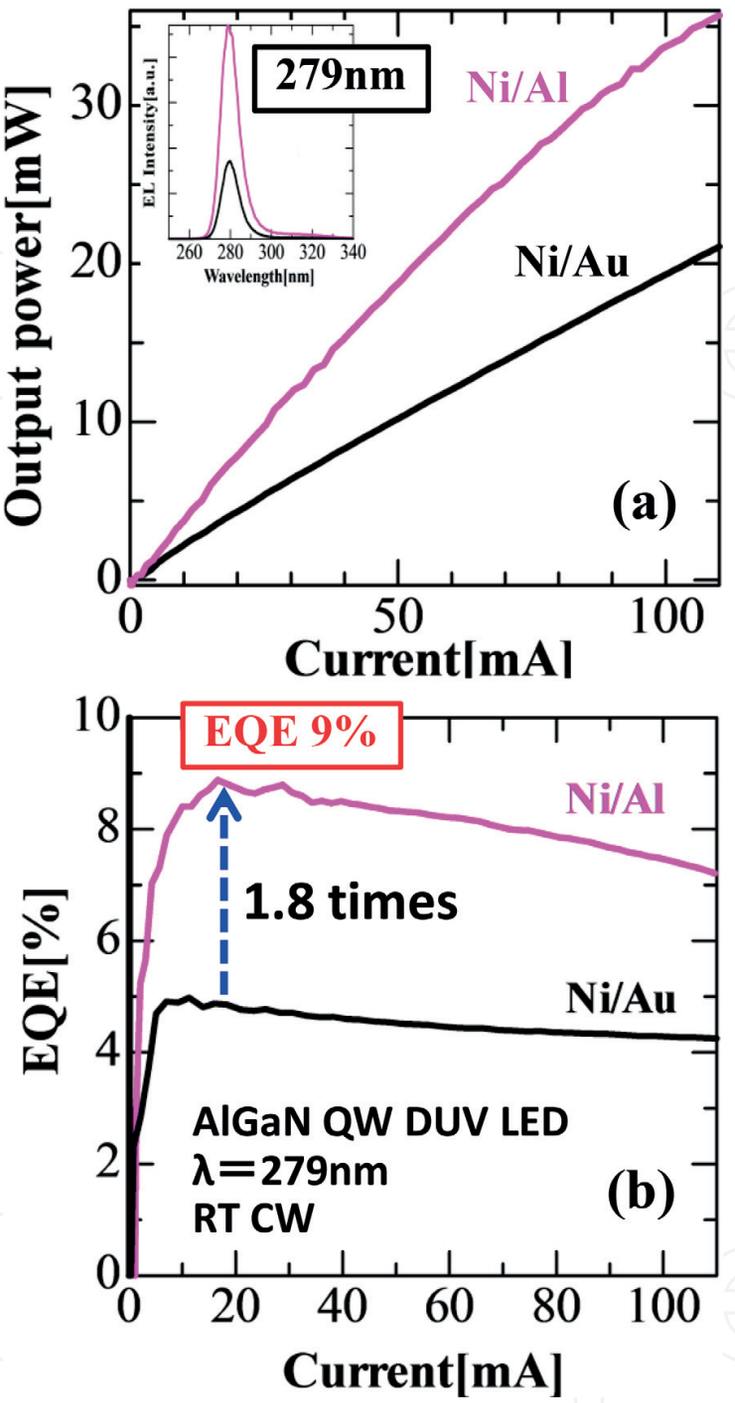

Figure 24. (a) Current-output power (I-L) and (b) current-EQE (η_{ext}) characteristics for 279 nm AlGaN-MQW DUV LEDs measured under cw operation at RT. comparison is made between LEDs with different p-type electrodes (conventional Ni/Au and highly reflective Ni/Al p-electrodes).

evaluated the transmittance of p-$Al_{0.65}Ga_{0.35}N$ prior to introducing it as a p-type contact layer. We confirmed almost perfect transparency for the p-AlGaN contact layer, and even the Mg doping concentration was as high as 8×10^{19} cm^{-3} as measured by secondary ion mass spectrometry (SIMS).

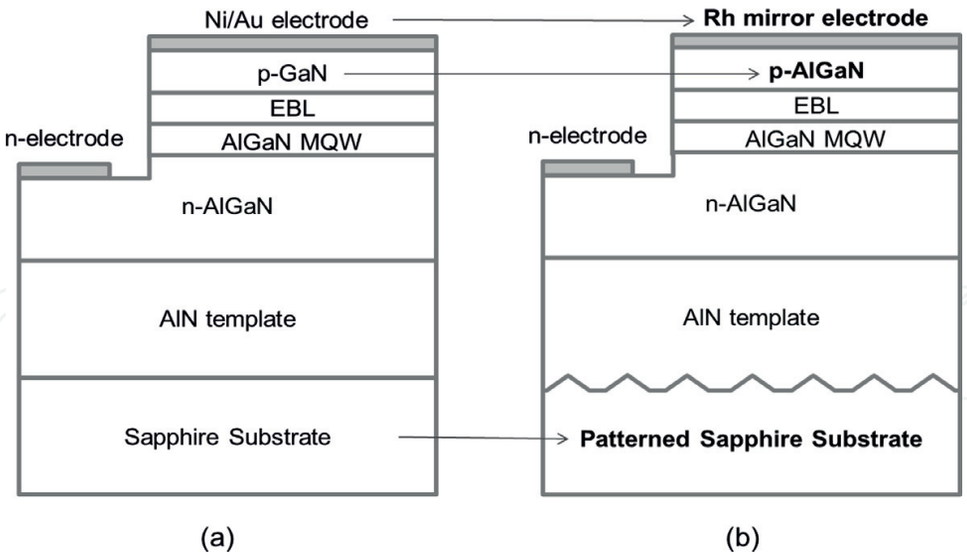

Figure 25. Schematics of (a) conventional and (b) LEE enhanced UV-LED structures. In the LEE enhanced UV-LED structure, we introduced a transparent p-type AlGaN:Mg contact layer, a Rh mirror electrode, a PSS, and an encapsulating resin.

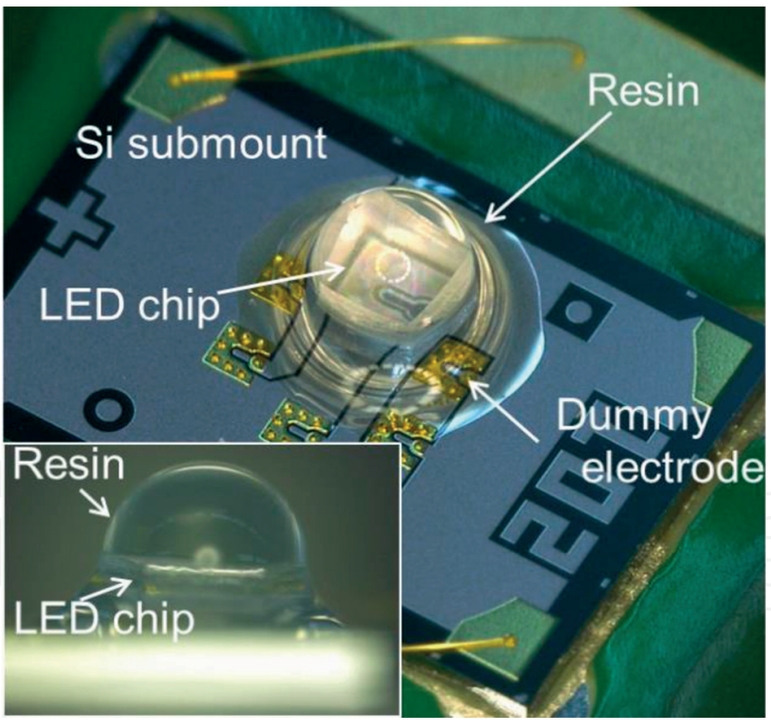

Figure 26. Photograph of the flip-chip (FC) LED mounted on a Si submount with an Al coating. The chip size is 0.5×0.5 mm^2 and it is encapsulated in resin with a hemispherical shape. The Si submount is in contact with the Al baseplate. The inset shows a side view of the encapsulating resin.

Figure 27(a) and **(b)** show the I-L and I-EQE characteristics for the conventional and LEE enhanced type UVC LEDs under RT cw operation. The inset in **Figure 27(a)** shows the EL spectra at 20 mA. Each spectrum has the same peak at 275 nm. The output power for both

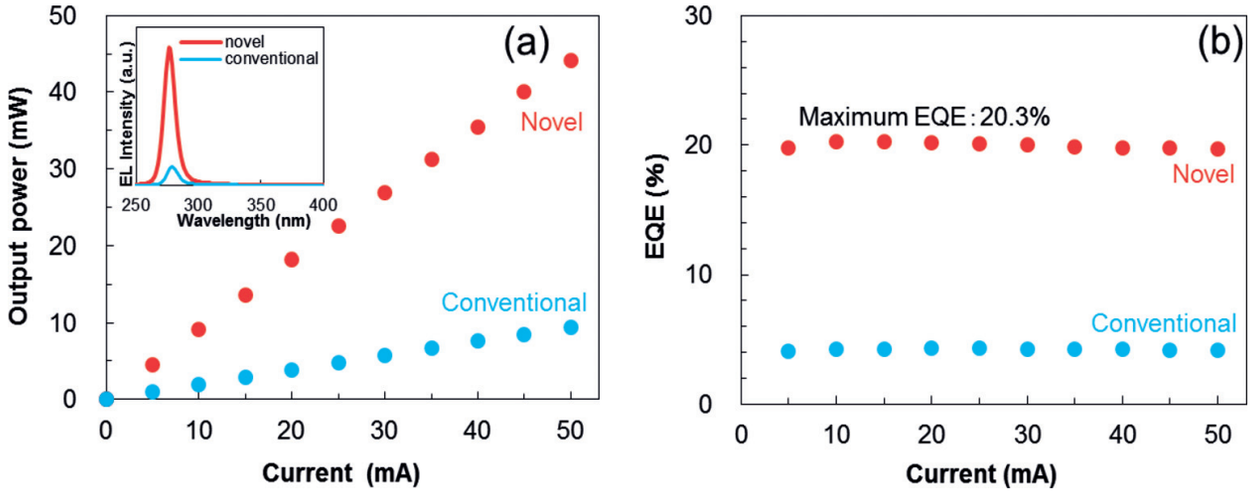

Figure 27. (a) Current-output power (I-L) and (b) current-EQE (η_{ext}) characteristics for the conventional and LEE enhanced UVC-LED. The inset in (a) shows the EL spectra of the LEDs at a direct current of 20 mA.

samples has good linearity, and the EQEs are almost constant up to 50 mA. The output power was increased from 3.9 to 18.3 mW at 20 mA and from 9.3 to 44.2 mW at 50 mA, both by a factor of five, by introducing LEE enhanced structure. These values correspond to EQEs of 4.3 and 20.3%, respectively. Thus, the EQE was substantially improved by including a transparent p-AlGaN contact layer, an Rh mirror electrode, a PSS, and the lens-like encapsulating.

To clarify the individual effects on the EQE, each structure for LEE enhancement was introduced step-by-step. **Table 2** summarizes the device structures and the LED characteristics. From **Table 2**, we found that the enhancement factors for introducing a transparent p-AlGaN contact layer and Rh electrode, PSS, and lens-like encapsulation were approximately 3, 1.5, and 1.5, respectively.

The driving voltage of the LED was increased from 9 to 16 V at 20 mA by introducing p-AlGaN contact layer. The main reason for the increase in driving voltage is the increase of contact resistant by introducing p-AlGaN contact layer. The WPE of the LEE enhanced type LEE

sample No.	Device structures				LED characteristics	
	substrate	p-type contact layer	p electrode	geometry	output power @20mA (mW)	maximum EQE(%)
1	flat	GaN:Mg	NiAu	FC only	3.9	4.3
2	flat	AlGaN:Mg	Rh	FC only	11.6	12.7
3	PSS	AlGaN:Mg	Rh	FC only	14.5	16.1
4	PSS	AlGaN:Mg	Rh	FC + resin coating	18.3	20.3

Table 2. Summary of the device structures and their LED characteristics. Samples no. 1 and 4 correspond to the conventional and novel UV-LED structures, respectively. Samples no. 2 and 3 demonstrate the effects of including the AlGaN:Mg/Rh layers and the PSS, respectively.

remained 5.7%. Improving the conductivity of the p-AlGaN contact layer is important issue in future for obtaining high WPE.

In summary of this section, LEE of the 275 nm AlGaN UVC LED was increased by approximately five times by introducing a transparent p-AlGaN contact layer, an Rh reflective electrode, a PSS, and a lens-like encapsulating. A maximum EQE of 20.3% at 275 nm was obtained by combining all of the aforementioned light extraction features.

8. Highly reflective (HR) PhC for increasing LEE

To improve the LEE of UVB and UVC LEDs, the introduction of a transparent contact layer and a highly reflective electrode is important as indicated in the previous section. A p-AlGaN layer with high Al composition (50–70%) is used for the transparent p-contact layer for UVC LEDs, however, the low hole concentration of this layer leads an increase in the contact resistance, resulting in a higher operating voltage.

In order to realize both high LEE and low voltage operation in DUV LEDs, we proposed using a highly-reflective photonic crystal (HR-PhC) [57–60]. It is possible to reflect UV light efficiently by using a 2-dimensional (2D) PhC on the surface of the p-GaN top contact layer. We can obtain low contact resistance because the top p-GaN layer has a high hole concentration. Therefore, a HR-PhC fabricated on p-GaN contact layer makes it possible to achieve not only high LEE but also high WPE in DUV LEDs.

It is possible to increase LEE by lens bonding or lens-shaped encapsulation [34, 56], or by fabrication of a PhC on the backside of the device for suppressing the total reflection [40]. However, LEE still remains low if we are unable to eradicate the strong absorption in the p-GaN layer.

We fabricated DUV LEDs with a HR-PhC on the p-AlGaN contact layer. The fabrication of a uniform PhC with low damage made it possible to obtain high EQE [57]. **Figure 28** shows a schematic structure of DUV LED with and without a HR-PhC region fabricated on the p-AlGaN contact layer. We used two-types of p-type electrodes, i.e., low-reflective (30%) Ni electrode and highly-reflective Ni(1 nm)/Mg (80%) [55] electrode.

We performed a finite-difference time-domain (FDTD) analysis for obtaining an appropriate HR-PhC design using the following Bragg equation [57]:

$$m\lambda/n_{eff} = 2a \tag{1}$$

where m is an integer, λ is the wavelength of the light, n_{eff} is the effective refractive index of the PhC, and a is the lattice period of the PhC. Electromagnetic field analysis by the FDTD method is suitable for analyzing structures with sub-wavelength size geometry, and is usually used for the analysis of optical PhC devices. An air hole-type 2D PhC with hexagonal configuration was assumed. We observe that a larger photonic bandgap is obtained with larger R/a, i.e., with $R/a = 0.4$, where R is the radius of the holes in the PhC. The values used in this work were $\lambda = 280$ nm, $n_{eff} = 2.3$, $m = 4$ and $a = 250$ nm [57–60].

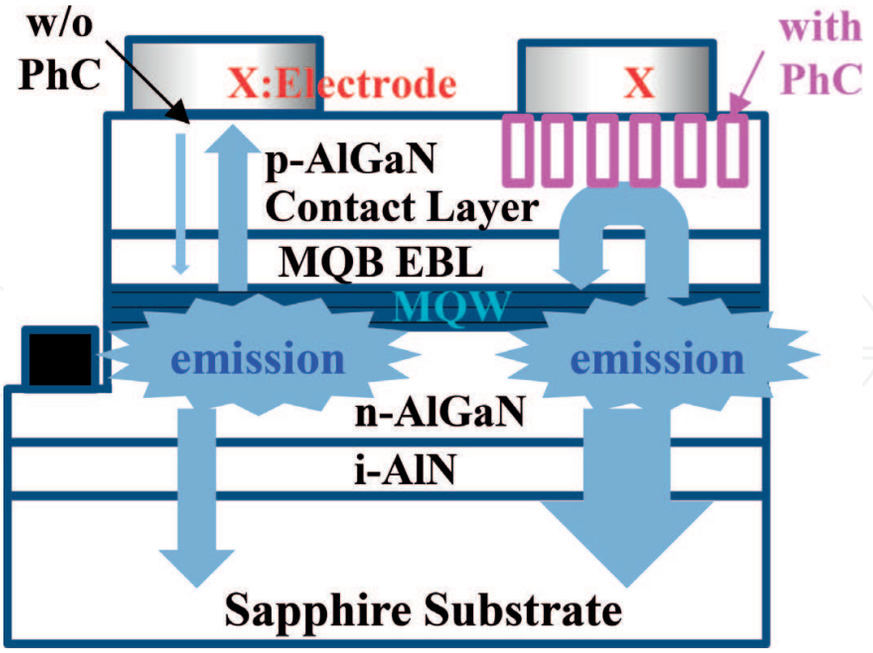

Figure 28. Schematic diagram of the structure of DUV LEDs with and without a reflective PhC on the p-AlGaN contact layer.

Figure 29 shows the schematic cross-sectional structures and electronic-field (E-field) mappings calculated by using FDTD method for 280 nm UVC LEDs (a) with and (b) without reflective HR-PhC, which is fabricated in the p-AlGaN/p-GaN contact layer. To obtain high reflectivity of UV radiation from the QW emitting region, we set the distance between the bottom of PhC air-rod and the QW to be 60 nm [57]. As can be seen in **Figure 29(b)**, the UV light from the QWs propagates equally in all directions for a usual Led case. On the other hand, if we introduce the HR-PhC, radiation from the QWs does not penetrate into the PhC, as shown in **Figure 29(a)**, resulting in realizing a highly-reflection of radiated light. From the FDTD analysis, we found that the LEE is increased by factors of approximately 2.8 and 1.8 at maximum by introducing the HR-PhC into the p-GaN and p-AlGaN contact layers, respectively. We also found that the LEE enhancement factor significantly depends on the value of R/a and that the appropriate R/a value is around 0.4 [57].

Based on these design, we fabricated DUV LEDs with HR-PhCs on the p-AlGaN contact layer. We used nano-imprinting and inductively-coupled plasma (ICP) dry-etching to fabricate a low-damage PhC. **Figure 30** shows (a) a cross-sectional scanning electron microscopy (SEM) image and (b) a high-resolution (HR) TEM image of the hexagonally configured PhC, as well as (c) surface and (d) cross-sectional SEM images of the Ni-electrode.

The period, diameter and depth of the air-holes were 252, 100 and 64 nm, respectively, confirmed by HR-TEM. Also, three-layer MQW and the 2-layer MQB-EBL located just below the air-holes of the PhC were observed in the HR-TEM. Finally, Ni and Ni/Mg electrodes were deposited via a tilted-evaporation method. We confirmed that the air-holes remained clear, with partial evaporation of Ni at the edges.

Figure 31 shows (a) the *I-L* and (b) the *I*-EQE characteristics of 283 nm AlGaN DUV LEDs with high-reflectivity Ni/Mg electrodes (reflectivity of >80%) with and without a PhC on the

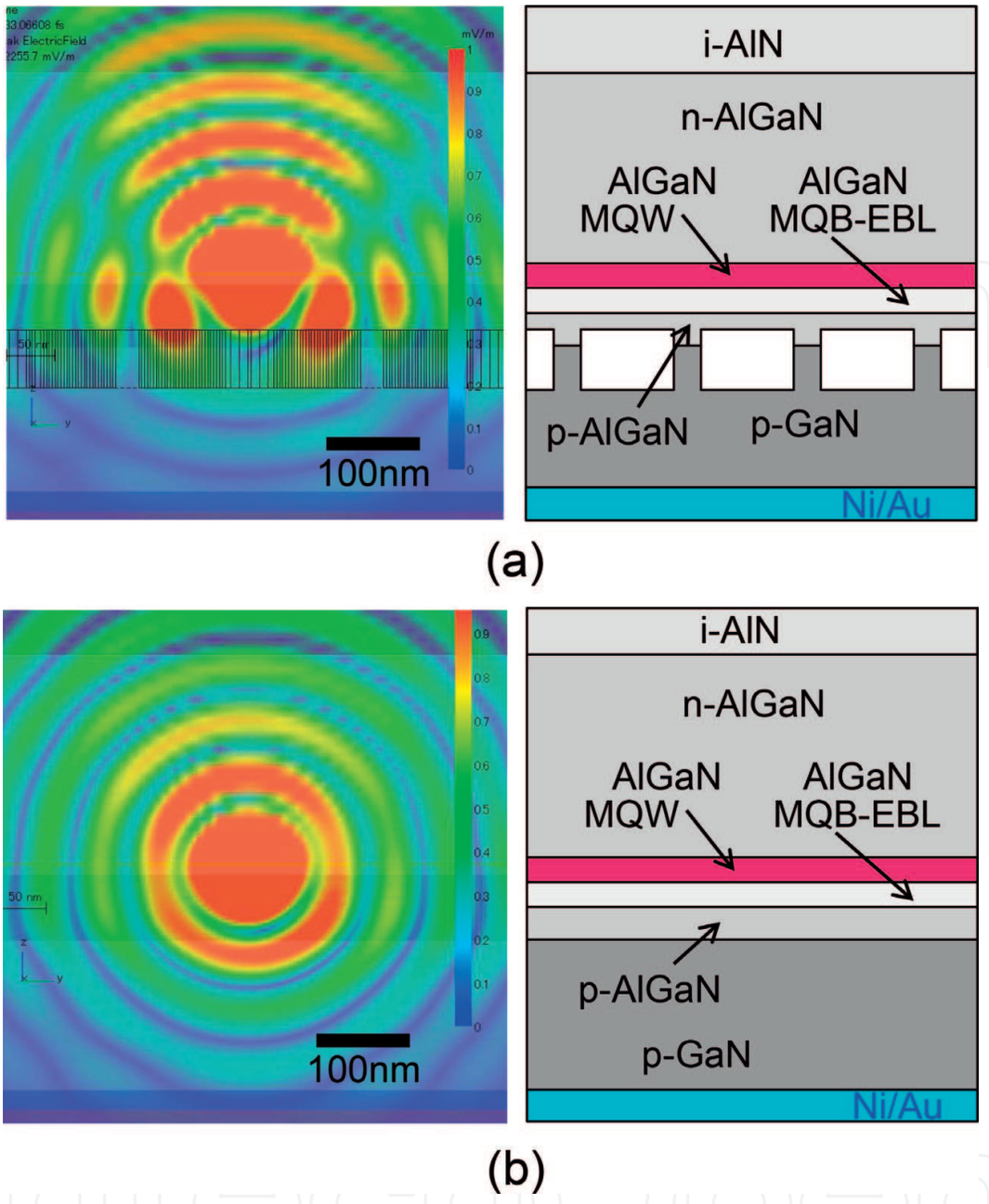

Figure 29. Cross-sectional structures and electronic-field mappings calculated by using FDTD method for 280 nm DUV LEDs (a) with and (b) without reflective PhC.

transparent p-AlGaN contact layer. The LEDs were measured under continuous wave operation on the bare wafers at room temperature. The maximum EQEs of the LEDs with and without the HR-PhC were 10 and 7.9%, respectively. The introduction of the PhC increased the EQE by a factor of 1.23, which is almost the same as obtained by FDTD simulation [57]. We also performed the same experiments using low-reflective Ni p-electrode, and obtained the maximum EQEs with and without the HR-PhC of 6 and 4.8%, respectively. The relatively low EQE of 4.8% is attributed to the low reflectivity of Ni. According to a simple estimate of the relationships between the EQEs of 4.8% (Ni; 30%), and 7.9% (Ni/Mg; 80%) for the LEDs without the PhC, the reflectance for the HR-PhC p-AlGaN with the Ni/Mg electrode is

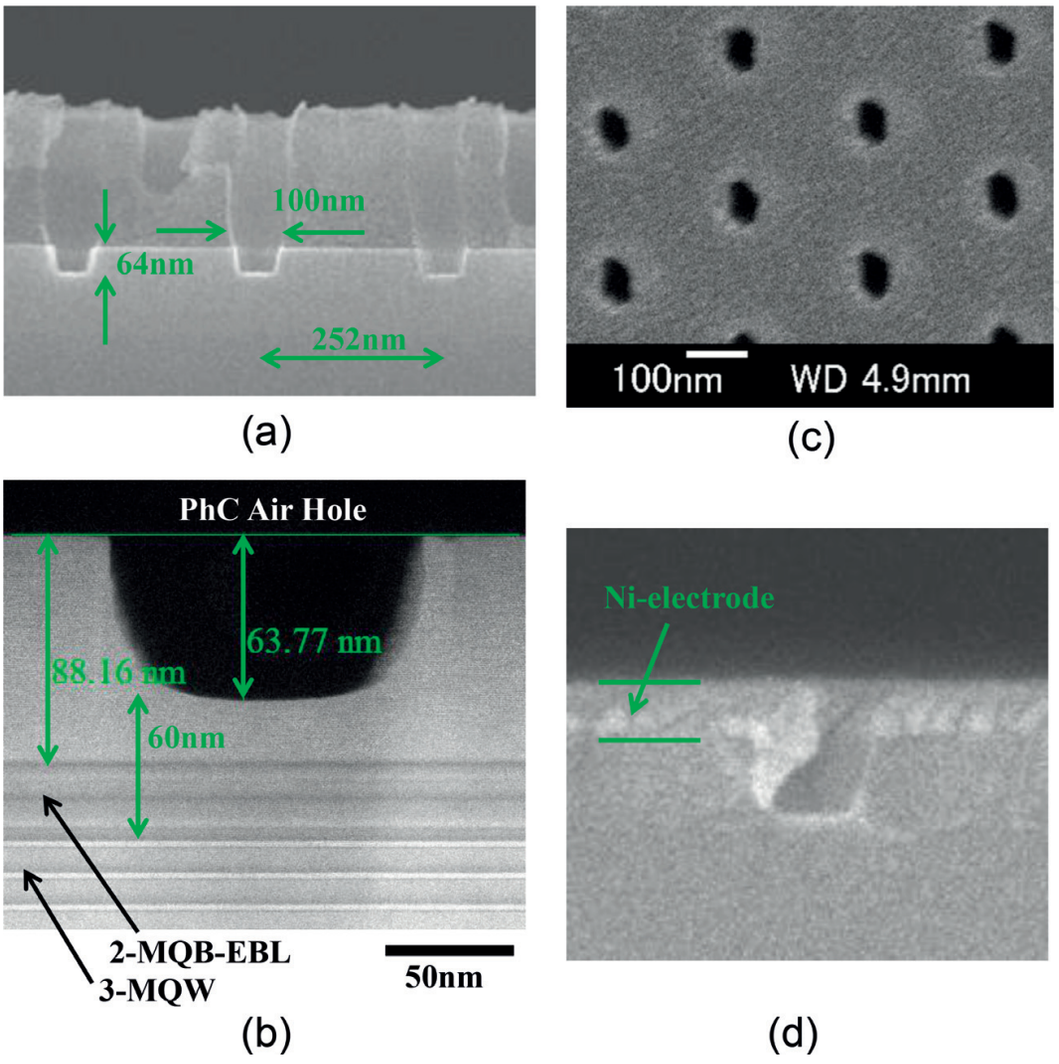

Figure 30. (a) Cross-sectional SEM and (b) HR-TEM images of the PhC fabricated on the p-AlGaN contact layer, along with (c) surface and (d) cross-sectional SEM images of a Ni electrode deposited on the PhC p-AlGaN layer by the tilted-evaporation method.

estimated to exceed 90%. These results indicate that the surface damage caused to the PhC during fabrication was negligible.

The value of *R*/*a* used in the experiments (*R*/*a* = 0.2) were not optimized value. If we had used a larger value of *R*/*a*, i.e., *R*/*a* = 0.4, we would have expected to obtain a significantly higher LEE. The LEE can be further increased by adopting FC technology and encapsulation. By introducing a PhC into the contact layer and reducing the operating voltage, it is expected that LEDs with higher WPE can be obtained.

9. Summary

We have demonstrated on the technologies to develop high-efficiency AlGaN-based DUV LEDs from the view point of increasing IQE, EIE and LEE. Significant increases in IQE of

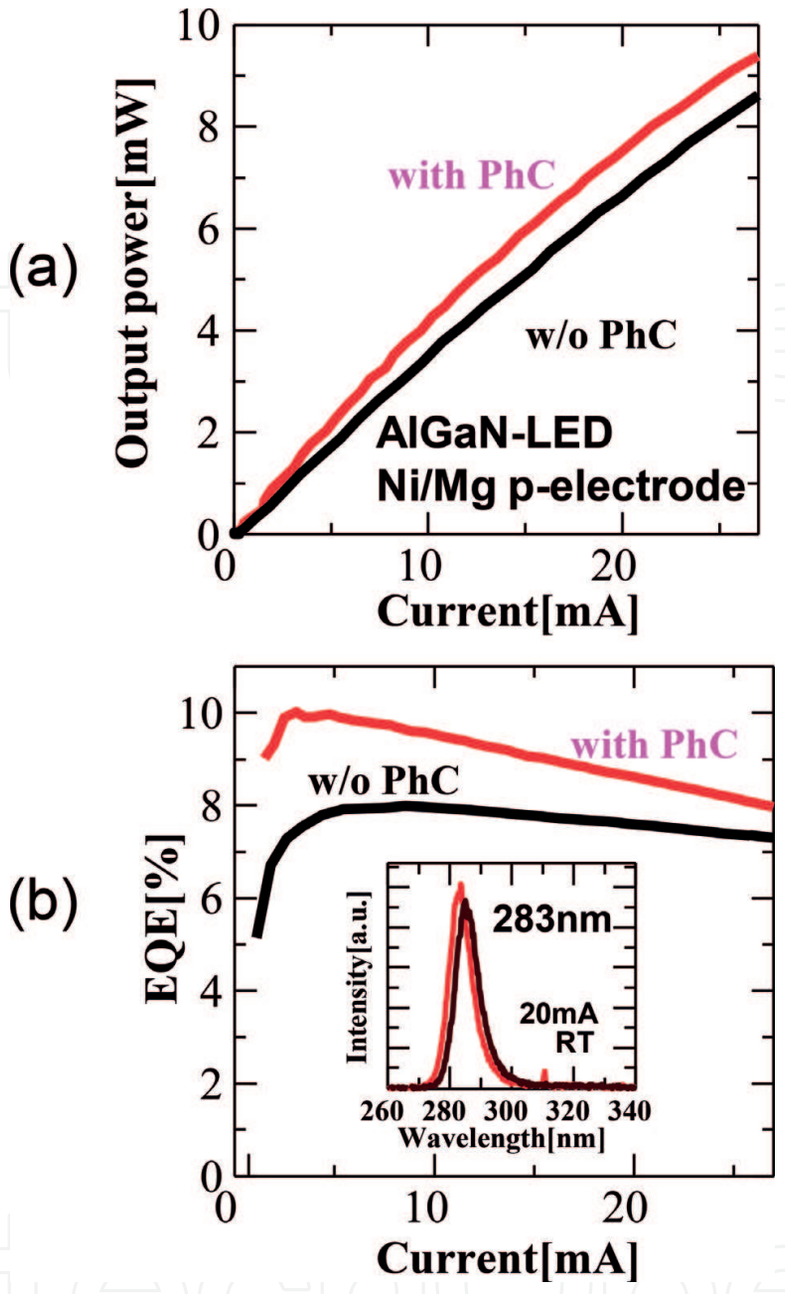

Figure 31. Comparison between the (a) I-L and (b) I-EQE characteristics of 283 nm AlGaN DUV LEDs with high-reflectivity Ni/Mg electrodes (reflectance of >80%) with and without a PhC on the transparent p-AlGaN contact layer.

DUV emission have been achieved for AlGaN-QWs by developing a low-TDD AlN layer grown on sapphire substrate. 222–351 nm DUV LEDs were made using this technology. The EIE of the LEDs was increased significantly by controlling the electron flow using an MQB. We also demonstrated improvements in LEE by using a transparent p-AlGaN contact layer, a highly reflective p-electrode, an AlN buffer layer on a PSS, and an encapsulating resin. The maximum EQE obtained was 20.3% for a 275 nm UVC LED, which is the highest EQE reported so far. We also demonstrated that an HR-PhC fabricated on the p-contact layer significantly increases the efficiency.

Author details

Hideki Hirayama

Address all correspondence to: hirayama@riken.jp

RIKEN, Wako, Saitama, Japan

References

[1] Hirayama H. Quaternary InAlGaN-based high-efficiency ultraviolet light-emitting diodes. Journal of Applied Physics. 2005;**97**:091101

[2] Kneissl M. III-nitride ultraviolet emitters. In: Springer Series in Material Science 227. Woodhead Publishing, ISSN 0933-033X; 2016

[3] Han J, Crawford MH, Shul RJ, Figiel JJ, Banas M, Zhang L, Song YK, Zhou H, Nurmikko AV. AlGaN/GaN quantum well ultraviolet light emitting diodes. Applied Physics Letters. 1998;**73**:1688

[4] Kinoshita A, Hirayama H, Ainoya M, Hirata A, Aoyagi Y. Room-temperature operation at 333 nm of Al0.03Ga0.97N/Al0.25Ga0.75N quantum-well light-emitting diodes with mg-doped superlattice layers. Applied Physics Letters. 2000;**77**:175

[5] Nishida T, Saito H, Kobayashi N. Efficient and high-power AlGaN-based ultraviolet light-emitting diode grown on bulk GaN. Applied Physics Letters. 2001;**79**:711

[6] Sun WH, Adivarahan V, Shatalov M, Lee Y, Wu S, Yang JW, Zhang JP, Khan MA. Continuous wave milliwatt power AlGaN light emitting diodes at 280 nm. Japanese Journal of Applied Physics. 2004;**43**:L1419

[7] Adivarahan V, Wu S, Zhang JP, Chitnis A, Shatalov M, Madavilli V, Gaska R, Khan MA. High-efficiency 269 nm emission deep ultraviolet light-emitting diodes. Applied Physics Letters. 2004;**84**:4762

[8] Adivarahan V, Sun WH, Chitnis A, Shatalov M, Wu S, Maruska HP, Asif Khan M. 250 nm AlGaN light-emitting diodes. Applied Physics Letters. 2004;**85**:2175

[9] Taniyasu Y, Kasu M, Makimoto T. An aluminium nitride light-emitting diode with a wavelength of 210 nanometres. Nature. 2006;**444**:325

[10] Hirayama H, Enomoto Y, Kinoshita A, Hirata A, Aoyagi Y. Efficient 230–280 nm emission from high-Al-content AlGaN-based multiquantum wells. Applied Physics Letters. 2002;**80**:37

[11] Hirayama H, Kinoshita A, Yamabi T, Enomoto Y, Hirata A, Araki T, Nanishi Y, Aoyagi Y. Marked enhancement of 320-360 nm ultraviolet emission in quaternary $In_xAl_yGa_{1-x-y}N$ with in-segregation effect. Applied Physics Letters. 2002;**80**:207

[12] Hirayama H, Enomoto Y, Kinoshita A, Hirata A, Aoyagi Y. Room-temperature intense 320 nm band ultraviolet emission from quaternary InAlGaN-based multiple-quantum wells. Applied Physics Letters. 2002;**80**:1589

[13] Hirayama H, Akita K, Kyono T, Nakamura T, Ishibashi K. High-efficiency 352 nm quaternary InAlGaN-based ultraviolet light-emitting diodes grown on GaN substrates. Japanese Journal of Applied Physics. 2004;**43**:L1241

[14] Fujikawa S, Takano T, Kondo Y, Hirayama H. Realization of 340-nm-band high-output-power (>7 mW) InAlGaN quantum well ultraviolet light-emitting diode with p-type InAlGaN. Japanese Journal of Applied Physics. 2008;**47**:2941

[15] Hirayama H, Yatabe T, Noguchi N, Ohashi T, Kamata N. 231–261 nm AlGaN deep-ultraviolet light-emitting diodes fabricated on AlN multilayer buffers grown by ammonia pulse-flow method on sapphire. Applied Physics Letters. 2007;**91**:071901

[16] Hirayama H, Yatabe T, Ohashi T, Kamata N. Remarkable enhancement of 254-280 nm deep ultraviolet emission from AlGaN quantum wells by using high-quality AlN buffer on sapphire. Physica Status Solidi C. 2008;**5**:2283

[17] Hirayama H, Noguchi N, Fujikawa S, Norimatsu J, Takano T, Tsubaki K, Kamata N. 222–282 nm AlGaN and InAlGaN-based deep-UV LEDs fabricated on high-quality AlN on sapphire. Physica Status Solidi A. 2009;**206**:1176

[18] Hirayama H, Tsukada Y, Maeda T, Kamata N. Marked enhancement in the efficiency of deep-ultraviolet AlGaN light-emitting diodes by using a multiquantum-barrier Electron blocking layer. Applied Physics Express. 2010;**3**:031002

[19] Hirayama H, Noguchi N, Yatabe T, Kamata N. 227 nm AlGaN light-emitting diode with 0.15 mW output power realized using a thin quantum well and AlN buffer with reduced threading dislocation density. Applied Physics Express. 2008;**1**:051101

[20] Hirayama H, Noguchi N, Kamata N. 222 nm deep-ultraviolet AlGaN quantum well light-emitting diode with vertical emission properties. Applied Physics Express. 2010;**3**: 032102

[21] Fujikawa S, Hirayama H, Maeda N. High-efficiency AlGaN deep-UV LEDs fabricated on a- and m-axis oriented c-plane sapphire substrates. Physica Status Solidi C. 2012;**9**(3–4):790-793

[22] Maeda N, Hirayama N. Realization of high-efficiency deep-UV LEDs using transparent p-AlGaN contact layer. Physica Status Solidi C. 2014;**10**:1521

[23] Hirayama H, Maeda N, Fujikawa S, Toyoda S, Kamata N. Development of AlGaN deep-UV LEDs with high light-extraction efficiency by introducing transparent layer structure. Optronics. 2014;**33**:58

[24] Hirayama H, Maeda N, Fujikawa S, Toyota S, Kamata N. Recent progress and future prospects of AlGaN based high-efficiency deep-ultraviolet light-emitting diodes. Japanese Journal of Applied Physics (Selected Topic). 2014;**53**:100209

[25] Mino T, Hirayama H, Takano T, Noguchi N, Tsubaki T. Highly-uniform 260 nm-band AlGaN-based deep-ultraviolet light-emitting diodes developed by 2-inch×3 MOVPE system. Physica Status Solidi C. 2012;**9**:749

[26] Mino T, Hirayama H, Takano T, Tsubaki K, Sugiyama M. Development of 260 nm band deep-ultraviolet light emitting diodes on Si substrate. Proceedings of SPIE. 2013;**8625**:59

[27] Shatalov M, Sun M, Bilenko Y, Sattu A, Hu X, Deng J, Yang J, Shur M, Moe C, Wraback M, Gaska R. Large chip high power deep ultraviolet light-emitting diodes. Applied Physics Express. 2010;**3**:062101

[28] Shatalov M, Sun W, Lunev A, Hu X, Dobrinsky A, Bilenko Y, Yang J. AlGaN deep-ultraviolet light-emitting diodes with external quantum efficiency above 10%. Applied Physics Express. 2012;**5**(8):082101

[29] Mickevičius J, Tamulaitis G, Shur M, Shatalov M, Yang J, Gaska R. Internal quantum efficiency in AlGaN with strong carrier localization. Applied Physics Letters. 2012; **101**(21):211902

[30] Moe CG, Garrett GA, Rotella P, Shen H, Wraback M, Shatalov M, Sun W, Deng J, Hu X, Bilenko Y, Yang J, Gaska R. Impact of temperature-dependent hole injection on low-temperature electroluminescence collapse in ultraviolet light-emitting diodes. Applied Physics Letters. 2012;**101**(25):253512

[31] Mickevičius J, Tamulaitis G, Shur M, Shatalov M, Yang J, Gaska R. Correlation between carrier localization and efficiency droop in AlGaN epilayers. Applied Physics Letters. 2013;**103**(1):011906

[32] Pernot C, Kim M, Fukahori S, Inazu T, Fujita T, Nagasawa Y, Hirano A, Ippommatsu M, Iwaya M, Kamiyama S, Akasaki I, Amano H. Improved efficiency of 255–280 nm AlGaN-based light-emitting diodes. Applied Physics Express. 2010;**3**(6):061004

[33] Inazu T, Fukahori S, Pernot C, Kim MH, Fujita T, Nagasawa Y, Hirano A, Ippommatsu M, Iwaya M, Takeuchi T, Kamiyama S, Yamaguchi M, Honda Y, Amano H, Akasaki I. Improvement of light extraction efficiency for AlGaN-based deep ultraviolet light-emitting diodes. Japanese Journal of Applied Physics. 2011;**50**(12R):122101

[34] Yamada K, Furusawa Y, Nagai S, Hirano A, Ippommatsu M, Aosaki K, Morishima N, Amano H, Akasaki I. Development of underfilling and encapsulation for deep-ultraviolet LEDs. Applied Physics Express. 2015;**8**(1):012101

[35] Grandusky JR, Gibb SR, Mendrick MC, Moe C, Wraback M, Schowalter LJ. High output power from 260 nm Pseudomorphic ultraviolet light-emitting diodes with improved thermal performance. Applied Physics Express. 2011;**4**:082101

[36] Grandusky JR, Chen J, Gibb SR, Mendrick MC, Moe C, Rodak L, Garrett GA, Wraback M, Schowalter LJ. 270 nm Pseudomorphic ultraviolet light-emitting diodes with over 60 mW continuous wave output power. Applied Physics Express. 2013;**6**:032101

[37] Kinoshita T, Hironaka K, Obata T, Nagashima T, Dalmau R, Schlesser R, Moody B, Xie J, Inoue S, Kumagai Y, Koukitu A, Sitar Z. Deep-ultraviolet light-emitting diodes fabricated

on AlN substrates prepared by hydride vapor phase epitaxy. Applied Physics Express. 2012; **5**:122101

[38] Kinoshita T, Obata T, Nagashima T, Yanagi H, Moody B, Mita S, Inoue S, Kumagai Y, Koukitu A, Sitar Z. Performance and reliability of deep-ultraviolet light-emitting diodes fabricated on AlN substrates prepared by hydride vapor phase epitaxy. Applied Physics Express. 2013;**6**:092103

[39] Kinoshita T, Obata T, Yanagi H, Inoue S. High p-type conduction in high-Al content mg-doped AlGaN. Applied Physics Letters. 2013;**102**:012105

[40] Inoue S, Tamari N, Taniguchi M. 150 mW deep-ultraviolet light-emitting diodes with large-area AlN nano-photonic light extraction structure emitting at 265 nm. Applied Physics Letters. 2017;**110**:141106

[41] Fujioka A, Misaki T, Murayama T, Narukawa Y, Mukai T. Improvement in output power of 280-nm deep ultraviolet light-emitting diode by using AlGaN multi quantum wells. Applied Physics Express. 2010;**3**:041001

[42] Ichikawa M, Fujioka A, Kosugi T, Endo S, Sagawa H, Tamaki H, Mukai T, Uomoto M, Shimatsu T. High-output-power deep ultraviolet light-emitting diode assembly using direct bonding. Applied Physics Express. 2016;**9**:072101

[43] Li XH, Detchprohm T, Kao TT, Satter MM, Shen SC, Yoder PD, Dupuis RD, Wang S, Wei YO, Xie H, Fischer AM, Ponce FA, Wernicke T, Reich C, Martens M, Kneissl M. Low-threshold stimulated emission at 249 nm and 256 nm from AlGaN-based multiple-quantum-well lasers grown on sapphire substrates. Applied Physics Letters. 2014;**105**(14):141106

[44] Mehnke F, Kuhn C, Stellmach J, Kolbe T, Ploch NL, Rass J, Rothe MA, Reich C, Ledenstov N, Pristovsek M, Wernicke T, Kneissl M. Effect of heterostructure design on carrier injection and emission characteristics of 295 nm light emitting diodes. Journal of Applied Physics. 2015;**117**(19):195704

[45] Susilo N, Hagedorn S, Jaeger D, Miyake H, Zeimer U, Reich C, Neuschulz B, Sulmoni L, Guttmann M, Mehnke F, Kuhn C, Wernicke T, Weyers M, Kneissl M. AlGaN-based deep UV LEDs grown on sputtered and high temperature annealed AlN/sapphire. Applied Physics Letters. 2018;**112**(4):041110

[46] Iida K, Kawashima T, Miyazaki A, Kasugai H, Mishima A, Honshio A, Miyake Y, Iwaya M, Kamiyama S, Amano H, Akasaki I. 350.9 nm UV laser diode grown on low-dislocation-density AlGaN. Japanese Journal of Applied Physics. 2004;**43**:L499

[47] Takano T, Narita Y, Horiuchi A, Kawanishi H. Room-temperature deep-ultraviolet lasing at 241.5 nm of AlGaN multiple-quantum-well laser. Applied Physics Letters. 2004;**84**:3567

[48] Ban K, Yamamoto J, Takeda K, Ide K, Iwaya M, Takeuchi T, Kamiyama S, Akasaki I, Amano H. Internal quantum efficiency of whole-composition-range AlGaN multiquantum wells. Applied Physics Express. 2011;**4**:052101

[49] Banal RG, Funato M, Kawakami Y. Optical anisotropy in [0001]-oriented $Al_xGa_{1-x}N$/AlN quantum wells (x>0.69). Physical Review B. 2009;**79**(R):121308

[50] Kawanishi H, Senuma M, Yamamoto M, Niikura E, Nukui T. Extremely weak surface emission from (0001) ***c***-plane AlGaN multiple quantum well structure in deep-ultraviolet spectral region. Applied Physics Letters. 2006;**89**:081121

[51] Iga K, Uenohara H, Koyama F. Electron reflectance of multiquantum barrier (MQB). Electronics Letters. 1986;**22**:1008

[52] Kishino K, Kikuchi A, Kaneko Y, Nomura I. Enhanced carrier confinement effect by the multiquantum barrier in 660 nm GaInP/AlInP visible lasers. Applied Physics Letters. 1991; **58**:1822

[53] Yun J, Hirayama H. Investigation of the light-extraction efficiency in 280 nm AlGaN-based light-emitting diodes having a highly transparent p-AlGaN layer. Journal of Applied Physics. 2017;**121**:013105

[54] Maeda N, Jo M, Hirayama H. Efficiency improvement of AlGaN deep UV-LEDs using highly-reflective Ni/Al p-type electrode. Physica Status Solidi A, in press. 2018

[55] Maeda N, Yun J, Jo M, Hirayama H. Enhancing the light-extraction efficiency of AlGaN deep-ultraviolet light-emitting diodes using highly reflective Ni/Mg and Rh as p-type electrodes. Japanese Journal of Applied Physics. 2018;**57**:04H08-1-04H08-4

[56] Takano T, Mino T, Sakai J, Noguchi N, Tsubaki K, Hirayama H. Deep-ultraviolet light-emitting diodes with external quantum efficiency higher than 20% at 275 nm achieved by improving light-extraction efficiency. Applied Physics Express. 2017;**10**:031002

[57] Kashima Y, Maeda N, Matsuura E, Jo M, Iwai T, Morita T, Kokubo M, Tashiro T, Kamimura R, Osada Y, Takagi H, Hirayama H. High external quantum efficiency (10%) AlGaN based deep-ultraviolet light-emitting diodes achieved by using highly reflective photonic crystal on p-AlGaN contact layer. Applied Physics Express. 2018;**11**:012101

[58] Kashima Y, Matsuura E, Kokubo M, Tashiro T, Ohkawa T, Hirayama H, Kamimura R, Osada Y, Shimatani S, Deep-UV LED device and its fabrication method, Japan Patent 5757512; 2015

[59] Kashima Y, Matsuura E, Kokubo M, Tashiro T, Ohkawa T, Hirayama H, Maeda N, Jo M, Kamimura R, Osada Y, Shimatani S, Deep-UV LED device and its fabrication method, Japan Patent 5999800; 2016

[60] Kashima Y, Matsuura E, Kokubo M, Tashiro T, Hirayama H, Kamimura R, Osada Y, Morita T, Deep-UV LED device and its fabrication method, Japan Patent 6156898; 2017